J. Fluid Mech. (1968), *vol.* 31, *part* 2, *pp.* 209–248
Printed in Great Britain

Gravity currents and related phenomena

By T. BROOKE BENJAMIN†

Institute of Geophysics and Planetary Physics,
University of California, La Jolla

(Received 4 April 1967)

This paper presents a broad investigation into the properties of steady gravity currents, in so far as they can be represented by perfect-fluid theory and simple extensions of it (like the classical theory of hydraulic jumps) that give a rudimentary account of dissipation. As usually understood, a gravity current consists of a wedge of heavy fluid (e.g. salt water, cold air) intruding into an expanse of lighter fluid (fresh water, warm air); but it is pointed out in § 1 that, if the effects of viscosity and mixing of the fluids at the interface are ignored, the hydrodynamical problem is formally the same as that for an empty cavity advancing along the upper boundary of a liquid. Being simplest in detail, the latter problem is treated as a prototype for the class of physical problems under study: most of the analysis is related to it specifically, but the results thus obtained are immediately applicable to gravity currents by scaling the gravitational constant according to a simple rule.

In § 2 the possible states of steady flow in the present category between fixed horizontal boundaries are examined on the assumption that the interface becomes horizontal far downstream. A certain range of flows appears to be possible when energy is dissipated; but in the absence of dissipation only one flow is possible, in which the asymptotic level of the interface is midway between the plane boundaries. The corresponding flow in a tube of circular cross-section is found in § 3, and the theory is shown to be in excellent agreement with the results of recent experiments by Zukoski. A discussion of the effects of surface tension is included in § 3. The two-dimensional energy-conserving flow is investigated further in § 4, and finally a close approximation to the shape of the interface is obtained. In § 5 the discussion turns to the question whether flows characterized by periodic wavetrains are realizable, and it appears that none is possible without a large loss of energy occurring. In § 6 the case of infinite total depth is considered, relating to deeply submerged gravity currents. It is shown that the flow must always feature a breaking 'head wave', and various properties of the resulting wake are demonstrated. Reasonable agreement is established with experimental results obtained by Keulegan and others.

CONTENTS

† On leave from the University of Cambridge.

1. Introduction

In this paper several hydrodynamical problems are studied mathematically, all of which relate more or less directly to gravity currents (or density currents, as they are often called) but which also relate to some analogous flow phenomena that are rather simpler in practical detail. Figure 1 depicts a gravity current as typically observed. Here a stream of heavy fluid is shown flowing along a horizontal bottom and displacing a fluid of smaller density. Due to the extra weight of the denser fluid, a larger piezometric pressure exists inside the current than in the fluid ahead, and this provides the motive force. The front of the current is generally observed to progress with nearly constant speed and to maintain the characteristic shape shown in the figure, so that evidently the motive force is balanced by a hydrodynamic drag—which may, of course, be partly accountable to friction along the bottom but whose main attribution in many cases is to momentum in the upper fluid. The latter idea, regarding the overall balance between horizontal momentum and hydrostatic force, is the leading theme throughout this paper.

The shape of the interface in figure 1 is copied from an experimental curve obtained by Keulegan (1958).† It is characterized by a 'head wave' which rises to a little over twice the mean height of the interface, and on the rearward side of which there is a highly turbulent zone suggestive of some kind of wave-breaking process. Further to the rear the interface becomes approximately horizontal. These outstanding features appear to be common to the many different physical phenomena that may be classed as gravity currents. Most of the available experimental studies have been concerned with the intrusion of salt water into an

† A curve with the same principal features but somewhat different proportions was presented by Ippen & Harleman (1952), having been obtained in unpublished experimental work by Braucher (1950). The difference between this and Keulegan's result was ascribed by Keulegan to wall effects, but it also might have been due to the fact that in his experiments the current (of salt water) was not as deeply submerged in the lighter fluid (fresh water). Comparable results have been obtained by Middleton (1966) and Wood (1966). An excellent photograph of a gravity current is to be found in the paper by von Kármán (1940) cited below: it is attributed to H. S. Bell.

expanse of fresh water, thus bearing directly on the important practical matter of locks that connect fresh-water canals to the sea. Submerged currents of muddy water (turbidity currents: e.g. see Keunen 1950) and avalanches of snow-laden air are other examples that can be included; and, as an example on a grand scale, there is the meteorological phenomenon of a 'cold front' where a current of cold air—perhaps further laden with dust stirred up from the ground—advances into a warm atmosphere (e.g. see Berson 1958; Clarke 1961). To admit an important sphere of practical application, a few words are needed qualifying the case of gravity currents moving downhill. Then the extra weight of the denser fluid

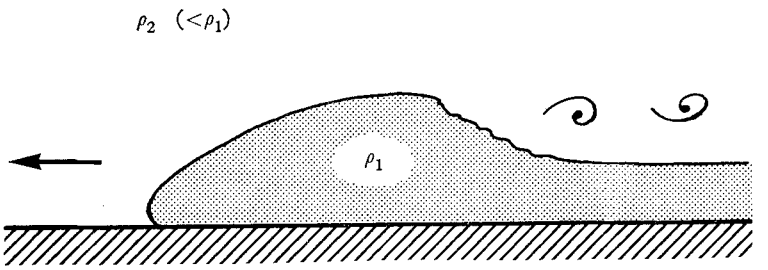

FIGURE 1. Observed form of gravity current (after Keulegan 1958).

contributes directly to the motive force; and the problem of flow along a horizontal bottom, as considered in this paper, is not strictly relevant. If the slope is fairly small, however, the front of the current is still driven primarily by hydrostatic pressure; thus the propagation speed is approximately independent of the slope, and the component of weight acting downhill is significant only in countering the frictional forces over a comparatively long stretch. Theory on the present basis would appear to have bearing on this further case, therefore, and indeed observation confirms that the front has the same characteristic form when the motion is down a slope of not more than a few degrees. A discussion of this aspect, citing some decisive observations reported recently by Middleton (1966), is included near the end of § 6.3.

A very simple theory of the initial motion at the front of a gravity current was suggested by Prandtl (1952, p. 369). He supposed that the mean flow velocity exceeds the velocity with which the front advances, so that part of the stream is deflected upwards at the front, forming a roll in a manner similar to the development of an incipient jet. Assuming that the heavier fluid in the roll does not fall back upon the current, and further neglecting the effect of hydrostatic forces, he deduced the ratio of the propagation velocity to the flow velocity by equating the dynamic pressures exerted by the two fluids against the front. This theory can only apply, of course, to a transient phase immediately following the release of a stream of heavier fluid into a deep expanse of lighter fluid—say, when a vertical sluice-gate separating masses of salt and fresh water is partially opened. Fairly soon the fluid that has been projected upwards falls upon and becomes entrained with the underlying current, so that a vigorously turbulent motion arises at the front; and this state in turn evolves into the final one of steady

propagation, where the turbulence is gathered behind the breaking head wave. Then the two velocities distinguished by Prandtl are necessarily the same.

A perfect-fluid model for steadily propagating gravity currents at great depths of submergence was discussed by von Kármán in part of a famous essay (1940, pp. 651, 652), and its essentials were reproduced in Yih's recent monograph (1965, p. 135). As shown in figure 2, the motion is viewed from a frame of reference travelling with the heavier fluid (of density ρ_1), which therefore appears to be at rest while the lighter fluid (of density ρ_2) appears to flow steadily over the interface, approaching from far ahead with the propagation velocity c_1. Accordingly von Kármán made two deductions on the basis of Bernoulli's theorem, in its form applicable to steady irrotational flows. First, by reasoning that recalled Stokes's deduction of the extreme, sharp-crested shape of water waves, he demonstrated the interesting property that the interface makes a sharp angle of 60° with the bottom at the forward stagnation point. Secondly, he applied the theorem between the stagnation point and points on the interface far downstream, supposing that the interface becomes horizontal there and that consequently the velocity of the flow along it tends to the constant value c_1. Thus he obtained a relation, equivalent to

$$c_1^2 = 2gH(\rho_1 - \rho_2)/\rho_2, \tag{1.1}$$

between the propagation velocity and the asymptotic height H of the interface above the bottom.

It is one of the main contentions of this paper, however, that von Kármán's argument leading to (1.1) must be repudiated, even though the same result is obtained by different reasoning in § 6.2. There are several precedents, outstandingly the theory of hydraulic jumps, to show that a condition of energy conservation may be an unjustifiable assumption for theoretical models of steady flows, and that generally a more fundamental condition is the overall balance of momentum fluxes against forces in the fluid. Thus a serious objection to the model illustrated in figure 2 is recognized, in that the suggested flow cannot possibly satisfy the latter condition—at least not when the lighter fluid is infinitely deep as supposed. For, if the interface is taken to become horizontal far downstream, a reckoning of the hydrostatic forces across two vertical sections respectively far upstream and downstream shows that a net force $\frac{1}{2}(\rho_1 - \rho_2)gH^2$ acts in the direction from right to left in the figure (i.e. this is the motive force remarked upon earlier). A steady state of flow cannot be realized unless such a force is balanced by a hydrodynamic drag manifested as a momentum deficiency in the receding stream; but this effect is clearly absent in the present instance, since the drag on any smooth 'half-body' in an irrotational flow of infinite expanse is exactly zero [see Prandtl & Tietjens (1934, § 78) for a proof regarding axisymmetrical half-bodies: the extension of their argument to plane flow is obvious]. It appears, therefore, that a wholly irrotational flow in the form suggested by figure 2 does not in fact exist: that is, in principle no such flow can be found satisfying the dynamical boundary condition that applies along the interface. From this conclusion one can well appreciate the fundamental reason for and inevitability of what is observed in practice, that the head wave breaks with

the production of much turbulence so that a wake is formed having the required momentum deficiency. These ideas are discussed further in §§ 6.2 and 6.4.

A good deal can nevertheless be learnt from simple models of this kind if, first, the fluid is given a fixed upper boundary at a finite height above the bottom and, secondly, allowance is made for the possibility of total head being lost. These aspects are examined in § 2, on the assumption that the flow becomes uniform far downstream. It is shown that a condition of energy conservation can hold only if the thickness h of the receding stream is half the total depth d; the case $h > \frac{1}{2}d$ is realizable with energy losses, but the case $h < \frac{1}{2}d$ is impossible since an external supply of energy would be necessary to sustain the flow. In § 3 the

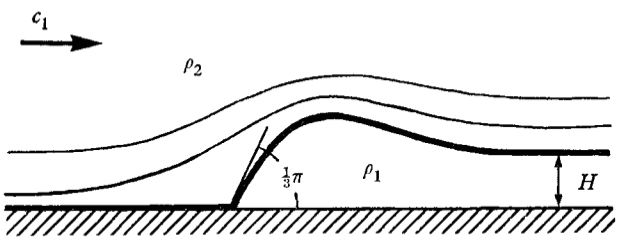

FIGURE 2. Theoretical model proposed by von Kármán.

wholly irrotational flow with $h = \frac{1}{2}d$ is studied in detail, and finally a close approximation to the form of the interface is obtained by the method of conformal transformation. This solution may be relevant to gravity-current experiments in which a partition initially separating salt and fresh water is suddenly withdrawn: each liquid then advances into the other in a wedge whose height is about half the total depth (Keulegan 1957; Yih 1965, p. 136, also 1947).†

There remains the more difficult question of whether irrotational-flow solutions exist featuring periodic waves downstream. Since the possibility appears that the resultant hydrostatic force might be balanced by wave-resistance, allowance for the formation of large-amplitude waves clearly revitalizes the theoretical model illustrated in figure 2. (In closing his discussion von Kármán prudently remarked that a mathematical solution to the suggested non-linear problem might be characterized by waves, though he did not recognize their significance as regards the equilibrium of the model.) The question is resolved in § 5 for the case of finite total depth, and in § 6.1 for the case of infinite depth. Somewhat contrary to expectation, the definite conclusion is that no wavy flow is in fact possible without a considerable loss of energy occurring. Thus the waveless flow already mentioned, in which the asymptotic level of the interface is midway between the horizontal boundaries of the system, is *unique* under the specification that the motion should be steady and irrotational everywhere.

† In this situation the ratio in question cannot be exactly half, however, since the speeds of the two wedges have to differ by a small fraction of the same order of magnitude as the fractional difference in the densities. But the results given in § 2 indicate that the total dissipation then occurring under conditions of steady propagation is of the same small order of magnitude, and so the assumption that energy is conserved should provide a good approximation. Thus there is no cause to dispute the validity of the estimate that Yih gives for the propagation speeds, which is based on this assumption.

Before the analysis is begun, a logical reduction of the problem to its simplest form needs to be introduced. We note that, with regard to the equilibrium of a steady motion, the same analytical problem is presented by a wedge of fluid displacing a heavier fluid from the under side of a horizontal plane. In the equations applicable respectively to this and to the original physical situation, the gravitational constant g will appear multiplied by a similar factor $\Delta\rho/\rho_2$, where $\Delta\rho$ is the positive density difference and ρ_2 is the density of the fluid approaching from ahead (the heavier fluid in the present case and the lighter in the original). Therefore no generality is lost by the theory if the density of the fluid in the wedge is taken to be insignificant in comparison with the density of the underlying fluid, so that the problem then relates to an empty or air-filled *cavity* displacing liquid beneath a horizontal boundary. A theoretical result obtained specifically for this analogous flow will apply to the other cases if g is replaced by $\hat{g} = g\Delta\rho/\rho_2$. The problem of flow past a cavity has considerable interest in its own right, and much of the physical discussion will be concerned with it.

2. The flow-force balance

Figure 3 illustrates the steady flow with a free boundary that, as was just explained, will be treated as the archetype for the class of flows in question. The density of the liquid is denoted by ρ, and the cavity is taken to be empty or filled with air whose weight is negligible. Viscosity and surface tension are ignored. Far upstream, where the liquid fills the space of depth d between the horizontal plane boundaries, the velocity c_1 of the flow is constant. Far downstream, the flow under the free boundary becomes uniform at depth h and velocity c_2. The possibility of wavy flows forming downstream will be examined later in § 5.

The object of this section is to show how the balance of flow force (i.e. momentum flux plus pressure force) between the approaching and receding parts of the stream determines the values of h/d and $c_1/(gd)^{\frac{1}{2}}$. In the first place the analysis is made on the supposition of no energy loss, which implies that the total head has the same value at all points of the flow. Then a simple model for a mechanism of energy loss is explored.

2.1. *Energy-conserving flow*

The point O in figure 3 is a stagnation point, and the pressure is zero everywhere along the free surface. Hence, by application of Bernoulli's theorem along this surface, it follows that

$$c_2^2 = 2g(d-h). \tag{2.1}$$

It also follows from the theorem that the pressure at the upper boundary far upstream is

$$p_0 = -\tfrac{1}{2}\rho c_1^2, \tag{2.2}$$

and the pressure in the liquid below has a hydrostatic variation with depth. The total pressure force (per unit span) acting across a section far upstream is therefore

$$p_0 d + \tfrac{1}{2}\rho g d^2 = \tfrac{1}{2}\rho(-c_1^2 d + g d^2), \tag{2.3}$$

the addition of which to the horizontal momentum flux $\rho c_1^2 d$ gives the flow force, thus

$$S_1 = \tfrac{1}{2}\rho(c_1^2 d + g d^2). \tag{2.4}$$

The pressure variation with depth is also hydrostatic far downstream, where the flow is again uniform. Hence another expression for the flow force is seen to be

$$S_2 = \rho(c_2^2 h + \tfrac{1}{2} g h^2). \tag{2.5}$$

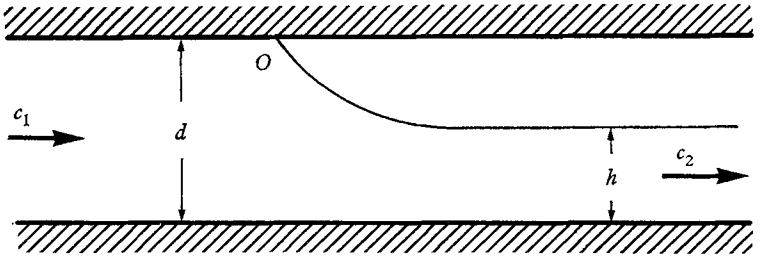

FIGURE 3. Specifications of analogous steady flow past a cavity.

But we must have $S_1 = S_2$, because the flow force is an invariant of any steady flow in the absence of external horizontal forces. Accordingly, coupled with the equation of continuity

$$c_1 d = c_2 h, \tag{2.6}$$

equations (2.4) and (2.5) lead to

$$c_2^2 = \frac{g(d^2 - h^2)d}{(2d - h)h}. \tag{2.7}$$

Comparing (2.1) and (2.7), we at once obtain a quadratic equation for h, one root of which is $h = d$ and the other is

$$h = \tfrac{1}{2} d. \tag{2.8}$$

Thus, in the only non-trivial case, the receding stream must occupy half the space between the planes if the flow is to be steady and free from energy dissipation. By the analogy explained in § 1, this result establishes also that a uniform gravity current can progress steadily without energy loss only if it fills half the space originally occupied by the lighter fluid.

Using the result (2.8), we find from (2.1) and (2.6) that

$$f = c_1/(gd)^{\frac{1}{2}} = \tfrac{1}{2}, \tag{2.9}$$

$$F = c_2/(gh)^{\frac{1}{2}} = \sqrt{2}. \tag{2.10}$$

It is of particular interest that the receding stream is supercritical (i.e. its Froude number $F > 1$). This fact tells us that stationary waves cannot arise upon the stream without energy loss, but a dissipative hydraulic jump may occur. This and other implications of (2.10) will be discussed later.

The flow that has just been determined may be realized very closely in the situation described by figure 4. Liquid initially fills a long rectangular box closed at both ends and fixed horizontally. One end is then opened, and under the action

of gravity the liquid flows out freely from this end. It can be expected that, after the transient effects of starting have disappeared, the air-filled cavity replacing the volume of the ejected liquid will progress steadily along the box. Observed in a frame of reference *travelling with the front of the cavity*, the motion of the liquid will appear to be steady, as shown in figure 3. If the effects of viscosity and surface tension are insignificant, therefore, the velocity of the cavity relative to a stationary observer will be c_1 as given by (2.9); and, since $h = \frac{1}{2}d$, the liquid will discharge from the open end with the same velocity.

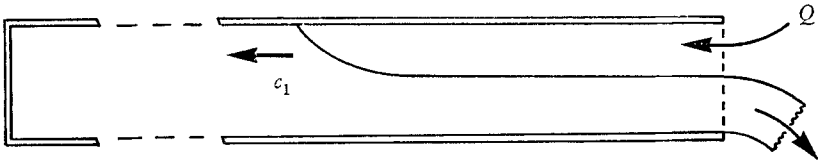

FIGURE 4. Illustration of the motion when liquid flows out from a long horizontal box.

The rate of discharge, being the same as the rate at which the volume of the cavity increases, is

$$Q = c_1(d-h) \tag{2.11}$$

per unit span, and this takes the value $\frac{1}{4}(gd^3)^{\frac{1}{2}}$ under the supposed conditions. Clearly, however, the parameter Q is amenable to some degree of experimental control: the flow of air into the lengthening cavity could be throttled, or the escape of liquid from the end could be impeded directly. There also appears the question whether higher rates of displacement by the advancing interface might be realizable by forcing air into the box (or correspondingly, in the analogous situation involving a gravity current, supplying the heavier fluid and removing the lighter at a rate higher than $\frac{1}{4}(\hat{g}d^3)^{\frac{1}{2}}$). To provide the flexibility that is needed in the theoretical model in order to make Q a disposable parameter, allowance has to be made for the possibility of energy dissipation.

[Before proceeding to the discussion of dissipational effects, we note a modification of the present results applying to gravity currents when, as is usual, the upper boundary (corresponding to the lower one for the cavity flow) is a free surface rather than a fixed plane as supposed. The ratio $\epsilon = \hat{g}/g = \Delta\rho/\rho_2$ is usually quite small, and this property ensures the approximate validity of the present theoretical model. However, it is straightforward to include the additional factor in the analysis: the total depth downstream then has to be treated as an extra variable, but the application of Bernoulli's theorem along the free surface gives another equation. The corrected form of the result (2.9) is found to be

$$f = c_1/(\hat{g}d)^{\frac{1}{2}} = \tfrac{1}{2}(1-\tfrac{9}{32}\epsilon), \tag{2.12}$$

if $O(\epsilon^2)$ is neglected. Similarly, the height H of the current (equivalent to $d-h$ in the unmodified model) is given by

$$H/d = \tfrac{1}{2}(1-\tfrac{15}{16}\epsilon). \tag{2.13}$$

Furthermore, it appears that above the current the free surface is depressed to a depth $\frac{3}{8}\epsilon d$ below its original level. The corrections $O(\epsilon)$ in (2.12) and (2.13) are

unlikely to be significant in the interpretation of experiments using salt water, since residual effects as small as this would probably be obscured by the effects of viscosity and of interfacial instability (see § 4.1). On the other hand, the depression of the free surface might be checked fairly accurately. The surface acts, in effect, as a water manometer indicating the increase in velocity head between the approaching and receding flows relative to the front of the current.]

2.2. *Flow with energy loss*

Use is to be made of the same device that serves in the elementary theory of hydraulic jumps (Lamb 1932, p. 280). It is supposed that the receding flow suffers a uniform loss of total head, so that its velocity c_2 far downstream is again uniform. Denoting the head loss by Δ, we then have in place of (2.1) that

$$c_2^2 = 2g(d-h-\Delta). \tag{2.14}$$

But equation (2.7) representing the balance of flow force is unaffected. Hence, equating the two expressions for c_2^2, we obtain directly

$$\Delta = \frac{(2h-d)\,(d-h)^2}{2h(2d-h)}. \tag{2.15}$$

This confirms that $\Delta = 0$ for $h = \frac{1}{2}d$, and further shows that Δ is positive for $h > \frac{1}{2}d$. Thus, steady flows where the receding stream fills more than half the space between the planes appear to be possible with energy losses. For $h < \frac{1}{2}d$, however, (2.15) shows Δ to be negative, which implies that an external supply of energy would be necessary to sustain a steady flow. We may conclude, therefore, that the case $h < \frac{1}{2}d$ is impossible in practice. An attempt to produce it in the way suggested near the end of § 2.1—that is, by pumping air into the cavity formed as liquid empties from a long box—would presumably be frustrated by entrainment of the extra volume of air in the stream of liquid issuing from the end of the box.

From (2.6) and (2.7) it follows that

$$\frac{c_1}{(gd)^{\frac{1}{2}}} = \left[\frac{h(d^2-h^2)}{d^2(2d-h)}\right]^{\frac{1}{2}}, \tag{2.16}$$

and hence, according to the definition (2.11) of Q,

$$\frac{Q}{(gd^3)^{\frac{1}{2}}} = \left[\frac{(d-h)^2h(d^2-h^2)}{d^4(2d-h)}\right]^{\frac{1}{2}}. \tag{2.17}$$

Figure 5 presents graphs of the dimensionless quantities Δ/d, $c_1/(gd)^{\frac{1}{2}}$ and $Q/(gd^3)^{\frac{1}{2}}$ plotted against h/d in the physically realizable range $0{\cdot}5 \leqslant h/d \leqslant 1$.

Note first from figure 5 that as h/d increases, $Q/(gd^3)^{\frac{1}{2}}$ falls steadily from its value $0{\cdot}25$ at $h/d = 0{\cdot}5$. Thus, the question raised near the end of § 2.1 is answered: in the situation illustrated in figure 4, the rate of displacement by the advancing free surface cannot be made larger than the value for free flow without energy loss.

Next note that the velocity c_1 (i.e. the velocity of propagation of the cavity in figure 4) at first increases with increasing h/d. The maximum value of $f = c_1/(gd)^{\frac{1}{2}}$ is found to be

$$f_m = 0{\cdot}5273, \tag{2.18}$$

and the corresponding value of h/d to be 0·6527. The form of the graph of $c_1/(gd)^{\frac{1}{2}}$ *vs.* h/d, showing that there are two possible values of the downstream depth for each value of the upstream velocity within a certain range, is easily understood upon reconsideration of the fact that in the energy-conserving flow ($h/d = 0{\cdot}5$) the receding stream is supercritical (i.e. $F = \sqrt{2} > 1$). By the allowance now made for dissipation, therefore, the receding stream may acquire

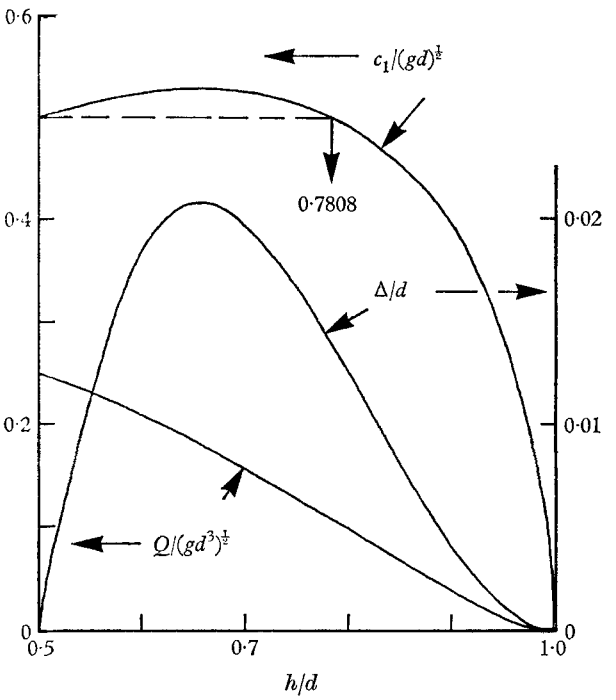

FIGURE 5. Graphs of non-dimensional propagation velocity $c_1/(gd)^{\frac{1}{2}}$, head loss Δ/d and cavity expansion rate $Q/(gd^3)^{\frac{1}{2}}$ considered as functions of h/d.

another possible, larger depth (and become subcritical) by passing through a hydraulic jump; and this second case is admitted by the flow-force balance throughout the range in which the first possible state of the receding stream remains supercritical. If h' is the first and h'' the second possible depth, then the familiar hydraulic-jump equations (e.g. see Lamb 1932, p. 280) show us that

$$h''/h' = \tfrac{1}{2}\{\sqrt{(1+8F^2)} - 1\}, \tag{2.19}$$

where $F = c_2/(gh')^{\frac{1}{2}}$. For example, considering the energy-conserving flow which has $h' = \frac{1}{2}d$ and $F = \sqrt{2}$, we obtain

$$h''/d = \tfrac{1}{4}(\sqrt{17} - 1) = 0{\cdot}7808. \tag{2.20}$$

This value is indicated in figure 5, to make the interpretation quite clear. Following this line of reasoning, we may conclude that

$$1 < F < \sqrt{2} \quad \text{for} \quad 0{\cdot}5 < h/d < 0{\cdot}6527,$$

$$F = 1 \quad \text{for} \quad h/d = 0{\cdot}6527 \quad (\text{when } c_1 \text{ is maximum}),$$

and

$$F < 1 \quad \text{for} \quad h/d > 0{\cdot}6527.$$

The head loss Δ is also found to have its maximum value ($= 0{\cdot}0209d$) for $h/d = 0{\cdot}6527$. Hence the rate of dissipation, given in practical units (e.g. ft. lb. sec^{-1} per ft. span) by

$$D = \rho c_1 d\Delta, \tag{2.21}$$

is maximum for this value of h/d. In figure 6, $D/\rho(gd^5)^{\frac{1}{2}}$ is plotted together with $c_1/(gd)^{\frac{1}{2}}$ and h/d against $Q/(gd^3)^{\frac{1}{2}}$, which, as was explained earlier with reference to figure 4, is the parameter amenable to direct experimental control. The optimum value of $Q/(gd^3)^{\frac{1}{2}}$, giving maxima of c_1, Δ and D, is 0·1831.

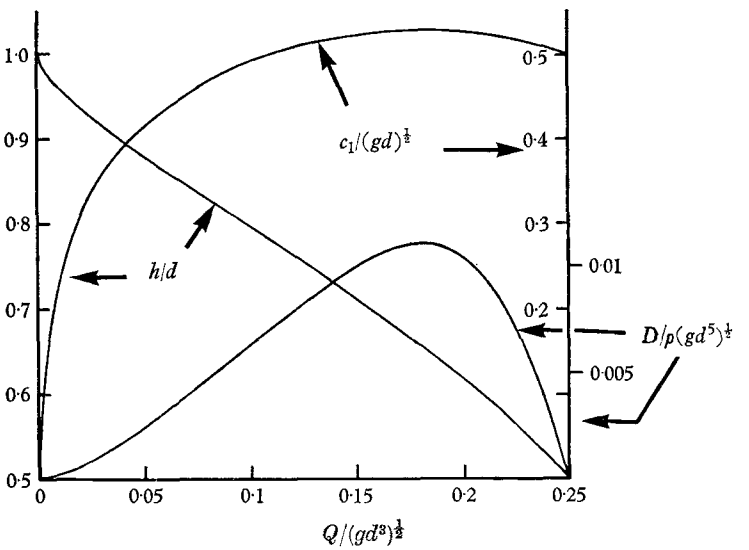

FIGURE 6. Graphs of h/d, $c_1/(gd)^{\frac{1}{2}}$ and $D/\rho(gd^5)^{\frac{1}{2}}$ considered as functions of $Q/(gd^3)^{\frac{1}{2}}$.

[Another result having interest with regard to the interpretation of gravity currents (see § 6.3) is the dimensionless coefficient of propagation velocity based on $H = d - h$. From (2.16) we obtain directly

$$C_1 = \frac{c_1}{(gH)^{\frac{1}{2}}} = \left[\frac{(d-H)(2d-H)}{d(d+H)}\right]^{\frac{1}{2}}, \tag{2.22}$$

which is plotted against H/d in figure 7.]

It seems likely that steady cavity flows with h/d in the open range between 0·5 and 0·6527 would be difficult, if not impossible, to produce experimentally. A slight reduction of $Q/(gd^3)^{\frac{1}{2}}$ below the 'free-inflow' value 0·25 would necessarily either make the flow unsteady or induce some dissipation, perhaps by breaking of the free surface and generation of turbulence, and this effect would probably precipitate the hydraulic jump that is possible. Thus, the receding flow would be forced into its alternative, subcritical condition corresponding to the established flow past the forward region of the free surface; and presumably the then superfluous part of Q (i.e. the excess above the value sufficient to sustain the second state of steady flow) would be taken up by air-entrainment far down-

stream. On the other hand, flows with $h/d \geqslant 0{\cdot}6527$ present no such contingency, and it appears probable that they can be produced quite optionally by controlling $Q/(gd^3)^{\frac{1}{2}}$ in the range from zero up to 0·1831.

The case when h/d approaches closely to 1 deserves comment, particularly since it relates to the important problem of a gravity current intruding into a very

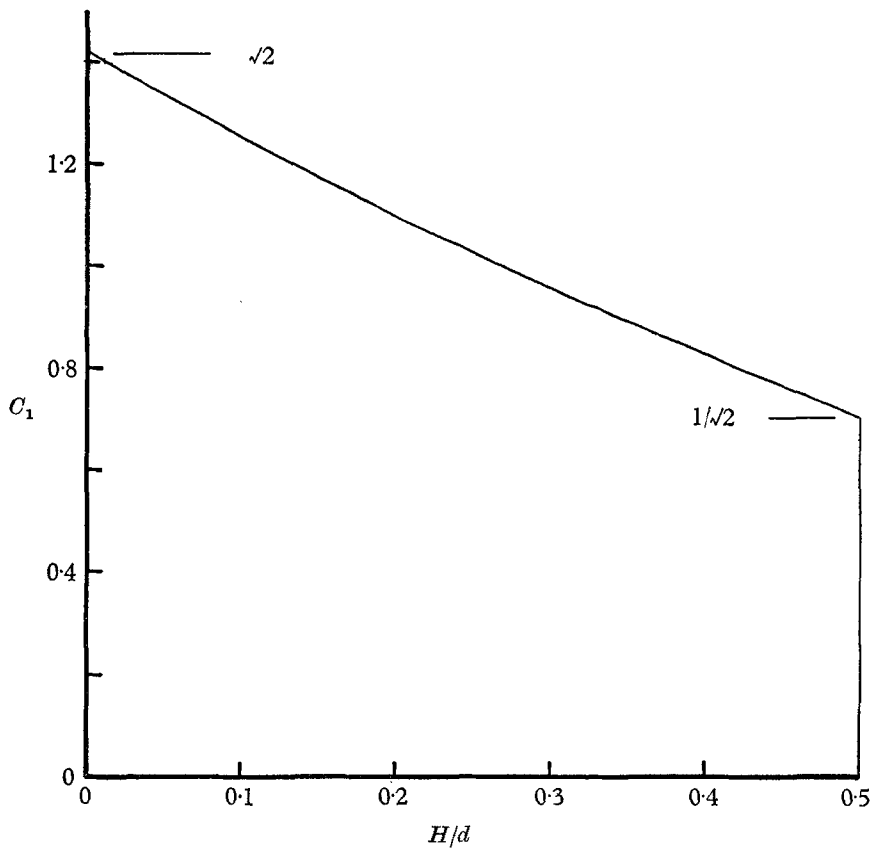

FIGURE 7. Graph of $C_1 = c_1/(gH)^{\frac{1}{2}}$ as a function of H/d.

deep expanse of fluid. Writing $H = d-h$, we find from the preceding results that $c_1 \to (2gH)^{\frac{1}{2}} \to (2gQ)^{\frac{1}{3}}$ as $d/H \to \infty$. It appears also that the head loss Δ vanishes in this limit, but the dissipation rate remains finite, that is,

$$D \to \rho(\tfrac{1}{2}gH^5)^{\frac{1}{2}} \to \rho(Q^5/16g)^{\frac{1}{3}}.$$

While the fact that the present model still predicts definite values of c_1 and D is reassuring, the application to this extreme case is open to serious objection, however, in that the assumption of a uniformly distributed head loss becomes totally unrealistic. In practice the loss will be confined to a region near the surface, probably of depth $O(H)$, and clearly this feature must be included in any theoretical model that is to be reliable. The matter will be taken up in § 6.

3. A three-dimensional problem: liquid emptying from a horizontal tube

This problem may be treated as one of steady motion, like the analogous two-dimensional problem solved in § 2.1. Its specifications are shown in figure 8. The cross-section of the tube is circular, with radius r, and the flow is assumed to be uniform far upstream and far downstream. The free surface far downstream subtends an angle 2α at the axis, so that its breadth is given by $b = 2r\sin\alpha$ and the cross-sectional area of the flow beneath it is given by

$$A = (\pi - \alpha + \tfrac{1}{2}\sin 2\alpha)r^2 = \pi r^2(1-\xi), \quad \text{say.} \tag{3.1}$$

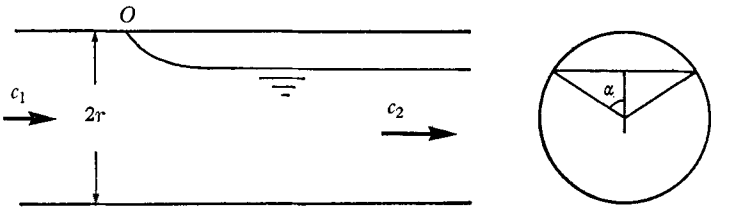

FIGURE 8. Specifications of cavity flow in horizontal tube of circular cross-section.

Hence the equation of continuity takes the form

$$c_1/c_2 = A/\pi r^2 = 1-\xi. \tag{3.2}$$

Applying Bernoulli's theorem along the free surface, between the stagnation point O and the asymptotic level far downstream, we obtain

$$c_2^2 = 2gr(1-\cos\alpha), \tag{3.3}$$

which is the counterpart of (2.1). And, rewriting (2.2), we again have that the pressure at the uppermost point of the cross-section far upstream is

$$p_0 = -\tfrac{1}{2}\rho c_1^2. \tag{3.4}$$

For a circular cross-section the centre of pressure is on the axis; hence the total pressure force is $(p_0+\rho gr)\pi r^2$. Thus, adding the momentum flux upstream, we have for the flow force

$$S_1 = (p_0+\rho gr+\rho c_1^2)\pi r^2 = \rho(gr+\tfrac{1}{2}c_1^2)\pi r^2. \tag{3.5}$$

Far downstream, where again the pressure variation with depth is hydrostatic, the total pressure force is given by

$$2\rho g r^3\int_\alpha^\pi (\cos\alpha-\cos\theta)\sin^2\theta\,d\theta = \rho gr(A\cos\alpha+\tfrac{2}{3}r^2\sin^3\alpha). \tag{3.6}$$

Hence an alternative expression for the flow force is

$$S_2 = \rho\{gr(A\cos\alpha+\tfrac{2}{3}r^2\sin^3\alpha)+Ac_2^2\}. \tag{3.7}$$

Putting $S_1 = S_2$ and using (3.2) and (3.3) to eliminate c_1 and c_2, we obtain after some reduction

$$\left.\begin{aligned}\xi^2(1-\cos\alpha)+\xi\cos\alpha-(2/3\pi)\sin^3\alpha = 0,\\ \text{in which}\qquad \xi = (\alpha-\tfrac{1}{2}\sin 2\alpha)/\pi.\end{aligned}\right\} \tag{3.8}$$

This equation for α has to be solved numerically. The only non-trivial and physically acceptable root is found to be $\alpha = 82{\cdot}78°$, for which $\xi = 0{\cdot}5978$. With this value of α, (3·3) gives

$$c_2/(gr)^{\frac{1}{2}} = 1{\cdot}322, \tag{3·9}$$

from which, using (3.2), we obtain finally

$$c_1/(gr)^{\frac{1}{2}} = 0{\cdot}767. \tag{3.10}$$

According to the same argument that was explained in § 2.1 with reference to figure 4, this result gives the speed of the advancing air-filled cavity formed when liquid flows freely out from one end of a horizontal tube.

The Froude number of the receding stream is properly defined by

$$F = c_2/C, \tag{3.11}$$

where C is the speed of long infinitesimal waves relative to the liquid. This definition preserves the significance of the Froude number in the ways that are well known respecting two-dimensional flows (for which $C = (gh)^{\frac{1}{2}}$): thus the expected condition $F > 0$ again means that the flow is supercritical and capable of forming a hydraulic jump. Using a formula for C implied by Lamb (1932, p. 256), we have

$$C = \left(\frac{gA}{b}\right)^{\frac{1}{2}} = \left\{\frac{\pi gr(1-\xi)}{2\sin\alpha}\right\}^{\frac{1}{2}} = 0{\cdot}996(gr)^{\frac{1}{2}}. \tag{3.12}$$

Hence (3.9) shows that

$$F = 1{\cdot}328, \tag{3.13}$$

which confirms that the receding stream is supercritical, though somewhat less so than in the corresponding two-dimensional problem (where $F = 1{\cdot}414$).

An excellent set of experimental results affording a comparison with the present theory was published recently by Zukoski (1966). Observing long bubbles as they propagated along tubes towards a closed end, he investigated extensively how their velocity was influenced by surface tension, viscosity and tube inclination. His findings are directly relevant in the case of horizontal tubes, where the experimental situation was essentially the same as that illustrated in figure 4. The importance of surface tension σ in the experiments was indicated by the size of a dimensionless parameter $\Sigma = \sigma/\rho gr^2$, the least value of which, $\Sigma = 0{\cdot}001$, was obtained using water as the liquid in a tube of 17.8 cm diameter. The effect of viscosity was shown to be insignificant in this instance. From Zukoski's figure 5, the corresponding measurement of the bubble velocity is seen to have been $c_1/(gr)^{\frac{1}{2}} = 0{\cdot}75$, which is only 2·2 % less than the theoretical result (3.10). Zukoski suggested (p. 833 of his paper) that the effect of surface tension remains important even at such small values of Σ, and that the velocity c_1 increases indefinitely in the limit $\Sigma \to 0$. However, this interpretation seems inadequately supported by the experimental data, and it seems unreasonable also on intuitive grounds. The alternative interpretation now proposed, which appears to be perfectly in keeping with the relevant data in Zukoski's figure 4, is that $c_1/(gr)^{\frac{1}{2}}$ approaches the predicted value 0·767 asymptotically as $\Sigma \to 0$.

Zukoski also made many experiments in which, instead of an air bubble, a

tongue of some different liquid advanced steadily along a horizontal tube, displacing the liquid that filled the tube up to the closed end. This phenomenon is an instance of a gravity current as we have defined it, and the present theory should again apply, subject merely to the adjustment that $\hat{g} = g\Delta\rho/\rho_2$ replaces g. In these experiments the effect of surface tension was dominant, however, as was indicated by larger values of $\Sigma = \sigma/\rho\hat{g}r^2$ and by the consistency of the relation between Σ and $c_1/(gr)^{\frac{1}{2}}$. Consequently, the observed velocities were substantially smaller than the present prediction.

The observed reduction in the velocity c_1 due to surface tension can readily be understood, although a definite estimate of it would be difficult to obtain theoretically since a rather complicated situation is presented in the neighbourhood of the forward stagnation point. There are two separate effects to be considered, which are best described with reference to the problems of steady motion indicated by figures 3 or 8. First, at the extreme front of the cavity, surface tension will act on its curved surface in such a way as to make the pressure inside higher than the stagnation pressure. Thus the formulae (2.1) or (3.3) would overestimate c_2^2, while (2.2) or (3.4) would overestimate p_0. Secondly, a contribution to the overall flow-force balance is made by the surface tension acting across a section through the flow far downstream. This may be partly counteracted by the streamwise component of contact forces at the forward edge of the cavity surface, but it is almost certainly never outweighed by the latter component. Thus, in effect, a positive quantity is subtracted from the expressions (2.5) or (3.7) for the downstream flow force S_2. Representing these two effects by implicit corrections to the equations mentioned and then evaluating the flow-force balance as before, one readily sees that both effects contribute to a reduction in c_1.

Zukoski further found in his experiments that bubbles would not propagate steadily along freely-emptying horizontal tubes if, owing to surface tension, $c_1/(gr)^{\frac{1}{2}}$ were reduced below about 0·5. He suggested—quite correctly, in the view of the present writer—that the change in behaviour is accountable to the receding flow becoming critical (i.e. $F = 1$). At higher propagation speeds the flow relative to the front of the bubble is supercritical downstream, which implies that small disturbances originating at the open end of the tube cannot overtake the bubble and therefore a steady régime must evolve. His argument regarding the magnitude of the relevant Froude number was admittedly very rough, however, and well-needed support is provided by the present definite result (3.13) showing that the receding flow is more than marginally supercritical in the absence of surface tension.

4. Further properties of the two-dimensional energy-conserving flow

We return now to the two-dimensional problem that was partly treated in § 2.1. There it was shown that if the steady flow depicted in figure 3 becomes uniform far downstream, then the asymptotic level of the free surface must be exactly halfway between the horizontal plane boundaries in order that the flow-force balance can be satisfied in the absence of dissipation. The implication of the flow-force balance in this case is that an irrotational flow does exist as sup-

posed, satisfying the condition of constant pressure everywhere along the free surface; and it will appear in § 5 that this waveless flow is the unique solution to the problem when the possibility of energy losses is excluded.

Three aspects of the flow are to be examined in this section. First, the application to gravity currents will be considered with regard to the stability of the interface. Secondly, it will be shown that there is no head wave as was featured in von Kármán's tentative model (see figure 2). Thirdly, in accordance with the latter deduction, an approximate expression will be derived for the complete form of the free surface.

4.1. *Stability*

When the flow is under an empty cavity, as shown in figure 3, the receding uniform stream is obviously stable to any small disturbance that the irrotational motion may suffer. (We are not concerned here with the possibility of hydraulic jumps or other large disturbances of an essentially dissipative character.) However, the property of stability is not preserved when, as was explained in § 1, the same flow model is applied to the description of gravity currents.

Consider first the application where the picture is the same as figure 3 but the space of the cavity is filled with stagnant fluid whose density ρ_1 is less than the density ρ_2 of the fluid flowing beneath the interface. The asymptotic depth h of the receding stream is again equal to $\frac{1}{2}d$, of course, and by scaling g appropriately in (2.1) we have that its velocity is given by

$$c_2^2 = 2gh(1-\gamma^{-1}), \tag{4.1}$$

where

$$\gamma = \rho_2/\rho_1 > 1. \tag{4.2}$$

To examine the stability of the asymptotic flow, we suppose in the usual way that the interface is slightly perturbed, so that its elevation η above the bottom is expressible in the form

$$\eta = h + a\,e^{i(kx-\omega t)}, \tag{4.3}$$

where x is the horizontal co-ordinate. By use of velocity potentials for the motions of the upper and lower fluids, a relationship between k and ω is easily found from the linearized kinematical condition and condition of pressure continuity at the disturbed interface. The details are not worth writing out since the required result can be inferred immediately from a result given by Lamb (1932, § 234, equation (8)). It is

$$\left\{\rho_1\left(c_2-\frac{\omega}{k}\right)^2+\rho_2\left(\frac{\omega}{k}\right)^2\right\}\coth kh = \frac{g}{k}(\rho_2-\rho_1), \tag{4.4}$$

which, after the substitution of (4.1) for c_2, can be rearranged to give

$$(\gamma+1)\,W^2-2\gamma W+\gamma\{1-\tfrac{1}{2}(kh)^{-1}\tanh kh\} = 0, \tag{4.5}$$

in which $W = \omega/kc_2$.

This result is the same whether ω or k is taken to be complex. Since the coefficients of the equation are real, it has either real or complex conjugate roots ω if k is a prescribed real wavenumber—and vice versa. Instability is indicated by the

existence of complex conjugate roots in either case: in the first, the root with $\mathrm{Im}\,(\omega) > 0$ implies there is a possible disturbance that is spatially periodic but everywhere grows exponentially with time; and in the second case, where the disturbance is understood to be periodic in time, the root with $\mathrm{Im}\,(k) < 0$ implies a disturbance growing with distance downstream. To deduce conditions of stability or instability, it is obviously sufficient to take the first case; thus we consider (4.5) as a quadratic equation for W corresponding to prescribed real values of k.

The condition under which (4.5) has real roots is that

$$kh \coth kh < \tfrac{1}{2}(\gamma+1), \tag{4.6}$$

and this is, therefore, both sufficient and necessary for stability. According to (4.6) there is a stable range of wavenumbers, $(0, k_c)$ say, whose upper limit k_c increases steadily with γ. The case of an empty cavity is represented by $\gamma \to \infty$, and so it is confirmed that there is then complete stability. At the other extreme when the densities of the two fluids are nearly equal, so that $\gamma \doteqdot 1$, the stable range of k is contracted towards zero, which means that all disturbances are unstable except those in the form of extremely long waves.

Let us next consider the application to a gravity current along the bottom. In the reference frame moving with the current, the lighter fluid (of density ρ_2) flows over the stagnant layer of heavier fluid (of density ρ_1); and by scaling (2.1) we now have that the velocity far downstream is given by

$$c_2^2 = 2gh(\gamma'-1), \tag{4.7}$$

where

$$\gamma' = \rho_1/\rho_2 > 1. \tag{4.8}$$

Hence the equation corresponding to (4.5) is found to be

$$(\gamma'+1)\,W^2 - 2W + 1 - \tfrac{1}{2}(kh)^{-1}\tanh kh = 0. \tag{4.9}$$

The condition for this equation to have complex conjugate roots W is that

$$kh \coth kh > (\gamma'+1)/2\gamma', \tag{4.10}$$

which is satisfied by all real values of k. Thus the flow is unstable to all possible small disturbances.

These simple conclusions are in accord with the results of more detailed analyses of interfacial instability that have been made by Keulegan (1949), Schijf & Schönfeld (1953) and others. Disturbances in the form of short waves, which lead to some mixing of the two fluids, are usually evident in experiments on gravity currents where the present energy-conserving condition applies approximately [e.g. certain of the experiments by Yih (1947) and Keulegan (1957): a good photograph of the phenomenon is presented in the paper by Ippen & Harleman (1952), though the circumstances were somewhat different from those considered here]. But generally these effects appear as only small-scale disfigurements of the theoretical flow, which is realized fairly clearly in the large. They definitely appear to have less overall importance than the effects of the wave-breaking process that arises when the energy-conserving condition is not satisfied (see §§ 5 and 6).

4.2. *Impossibility of a head wave*

A head wave is a characteristic feature of deeply submerged gravity currents in practice, and this feature was assumed in the perfect-fluid model that was proposed by von Kármán (1940; see also Yih 1965, p. 135). In his discussion of the model von Kármán wrote, 'It can also be shown analytically that the front of the heavy fluid must have a so-called *head*, whose peak is considerably higher than the mean thickness of the heavy layer'. Thus there is good reason to enquire

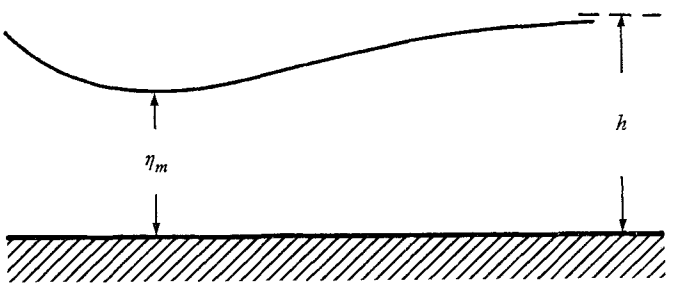

FIGURE 9. Illustration of contemplated flow featuring a head wave.

whether the present energy-conserving flow features a head wave, which would be a wave of depression, of course, in the archetypal model of cavity flow. The situation in view is depicted in figure 9. Here the free surface falls to a minimum level, below which the depth of the stream is η_m, and thereafter rises to the asymptotic level that we know it must take far downstream.

The conclusion that this situation is impossible in the absence of energy losses follows from a theorem given by Southwell & Vaisey (1946, p. 125; see also Binnie 1952), who attributed it to Allen. Regarding any steady two-dimensional flow along a horizontal open channel, the theorem states that the free surface can nowhere fall below the lower of the two possible 'asymptotic levels' fixed by the values of the discharge and total head. The higher level is that of a subcritical uniform stream, whereas the lower is that of a supercritical one.† Hence the impossibility of a head wave as depicted in figure 9 is established, since from (2.10) we have $F = c_2/(gh)^{\frac{1}{2}} = \sqrt{2}$ for the asymptotic flow.

Southwell & Vaisey's demonstration of the theorem is not the simplest possible, nor is Binnie's and neither is entirely precise. It seems worth while, therefore, to include the following short demonstration, which refers to figure 9.

Since the flow is irrotational, the square of the resultant velocity, $q^2 = u^2 + v^2$, cannot be a maximum at any point in the interior of the fluid (Lamb 1932, § 37).

† The respective depths η of the two flows are the two positive roots of

$$f(\eta) = \eta^3 - \eta^2 d + \mathcal{Q}/2g = 0,$$

in which $8gd^3 > 27\mathcal{Q}^2$. This cubic equation is simply a rearrangement of the definition of the total head d when the flow velocity is expressed by $u = \mathcal{Q}/\eta$, where $\mathcal{Q}$ is the discharge. We have $f' = 0$ and $f < 0$ for $\eta = \frac{2}{3}d$, which is the depth of a *critical* flow with the given d; i.e. this is the depth for which $F^2 = u^2/g\eta = 2(d-\eta)/\eta$ would be unity. It follows at once that one of the positive roots is larger and the other smaller than $\frac{2}{3}d$, and hence respectively $F < 1$ and $F > 1$ as stated above.

Applied along the free surface, Bernoulli's theorem shows that q^2 is largest at the lowest point of the surface, and its value there is

$$q_m^2 = c_2^2 + 2g(h - \eta_m). \tag{4.11}$$

Hence either q_m^2 is the largest value acquired by q^2 anywhere in the flow, or there is a larger value on the bottom. But the second possibility is excluded because the bottom is horizontal. Thus $v = 0$ everywhere along it and so, by the condition of zero vorticity, $\partial u/\partial y = \partial v/\partial x = 0$. Therefore q^2 will increase above the bottom if $\partial^2 u/\partial y^2 > 0$ or, which is the same thing since u in an irrotational flow is a harmonic function, $\partial^2 u/\partial x^2 < 0$. Because this condition is satisfied at the point where the velocity along the bottom is a maximum, it follows that still larger velocities occur in the interior of the fluid. Thus we can assert that, except at the lowest point of the free surface, q is everywhere smaller than q_m and *a fortiori* the magnitude of any single velocity component is smaller than q_m.

Now, evaluation of the discharge alternatively far downstream and at the minimum section shows that

$$c_2 h = \int_0^{\eta_m} u\, dy < q_m \eta_m, \tag{4.12}$$

where the inequality is an obvious consequence of the fact established immediately above. Combining (4.12) with (4.11) and cancelling a factor $h - \eta_m$, we obtain finally

$$2\eta_m^2 > F^2 h(h + \eta_m), \tag{4.13}$$

which shows that the supposition $\eta_m < h$ would be admissible only if $F < 1$. This proves the theorem.

It has been shown that a head wave cannot occur in the energy-conserving flow specified in § 2.1, and thus the free surface must fall steadily towards its asymptotic level. We may conclude that the head wave commonly observed at the front of gravity currents is essential, not merely incidental, to the dissipative process that becomes necessary when $h \neq \frac{1}{2}d$.

4.3. *Form of the free surface*

The general difficulties posed by problems of free-boundary flow under gravity are notorious. There is no known method of exact solution, and analytical methods of successive approximation are formidably complicated. If a limited but practically quite adequate standard of precision is accepted, however, an approximate solution to the present complete problem may be obtained fairly simply as follows. The principle of the method, which has been used before for similar problems, is to choose the unknown form of the free boundary in the hodograph plane, and to adjust its consequent form in the physical plane so that the non-linear boundary condition on it is satisfied as closely as possible.

Use will be made of the conformal mappings shown in figure 10. First, in figure 10 (*a*), the physical plane is represented as an Argand diagram of the complex variable $z = x + iy$, with the origin at the stagnation pcint O. It is convenient now to take c_1 as the unit of velocity and d as the unit of length, so that the asymptotic depth and velocity of the receding stream are respectively $\frac{1}{2}$ and 2 in

these units. Also, as shown by (2.9) or (2.10), g has the value 4. Hence along the free surface Bernoulli's equation takes the form

$$q^2 = u^2 + v^2 = -8y. \tag{4.14}$$

Next, figure 10(*b*) shows the mapping of the flow as an infinite strip in the plane of $w = \phi + i\psi$, where ϕ is the velocity potential and ψ the stream-function.

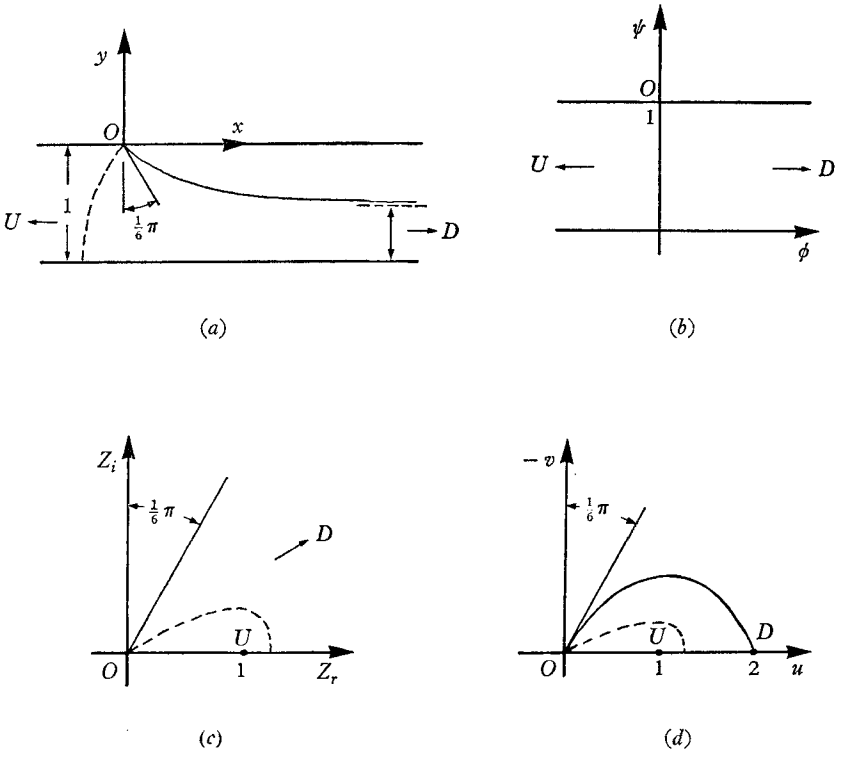

FIGURE 10. Conformal mappings of energy-conserving flow: (*a*) physical plane, $z = x + iy$; (*b*) plane of complex potential, $w = \phi + i\psi$; (*c*) plane of auxiliary variable, Z; (*d*) hodograph plane, $\zeta = u - iv$.

The horizontal bottom ($y = -1$) is chosen to be the streamline $\psi = 0$, and so the upper boundary including the free surface is the streamline $\psi = 1$. The equipotential $\phi = 0$ is chosen to be the one through O, and its mappings in the other planes are sketched as dashed lines.

For reasons that will appear presently, we need the transformation

$$Z = (e^{\pi w} + 1)^{\frac{1}{3}}, \tag{4.15}$$

which, as shown in figure 10(*c*), maps the flow in an infinite segment whose included angle is $\frac{1}{3}\pi$. The stagnation point ($w = i$) is represented by $Z = 0$, the uniform flow far upstream ($\phi \to -\infty$) by $Z = 1$, and the uniform flow far downstream ($\phi \to \infty$) by $|Z| \to \infty$ inside the segment. The free surface ($\phi > 0$, $\psi = 1$) is mapped along the radius $Z = |Z| \exp(\frac{1}{3}\pi i)$.

Now consider the complex variable

$$\zeta = \frac{dw}{dz} = u - iv. \tag{4.16}$$

The ζ-plane (hodograph) is shown in figure 10(*d*), and we can specify the following definite features of it, the first three of which are obvious and the fourth is a consequence of the fact recalled in § 1 from von Kármán's discussion (1940):

(i) O is mapped on $\zeta = 0$.

(ii) The flow infinitely far upstream ($Z = 1$) is mapped on $\zeta = 1$.

(iii) The flow infinitely far downstream ($|Z| \to \infty$) is mapped on $\zeta = 2$.

(iv) At the origin the curve mapping the free surface makes an angle $\frac{1}{3}\pi$ with the real axis. Thus the mappings ζ and Z overlap at the origin, and so

$$\zeta \sim aZ \quad \text{for} \quad |\zeta| \to 0, \tag{4.17}$$

where a is a positive real constant.

To find the value of a, we first put $w = i + w'$ in (4.15) and obtain

$$Z \sim \pi^{\frac{1}{3}} e^{\frac{1}{3}\pi i} (w')^{\frac{1}{3}} \quad \text{for} \quad |w'| \to 0. \tag{4.18}$$

When (3.17) and (3.18) are combined and ζ is written as dw'/dz, an integration then gives

$$(w')^{\frac{2}{3}} \sim \tfrac{2}{3} a \pi^{\frac{1}{3}} e^{\frac{1}{3}\pi i} z.$$

Hence

$$w' \sim (\tfrac{2}{3}a)^{\frac{3}{2}} \pi^{\frac{1}{2}} e^{\frac{1}{2}\pi i} z^{\frac{3}{2}}. \tag{4.19}$$

As expected, this describes the flow past the corner of $\frac{2}{3}\pi$ included angle made by the upper bounding streamline at O in the physical plane (cf. Lamb 1932, pp. 69, 418). Differentiating (4.19) to obtain ζ as a function of z, we have finally

$$q^2 = |\zeta|^2 \sim \tfrac{2}{3} a^3 \pi |z|,$$

or

$$q^2 \sim -(4/3\sqrt{3}) a^3 \pi y \tag{4.20}$$

along the free surface where $|z| = -y \operatorname{cosec} \frac{1}{3}\pi = -(2/\sqrt{3})y$. These steps in effect retrace backwards von Kármán's demonstration that the dynamical boundary condition fixes the angle of the free surface at the stagnation point; but on comparing (4.20) with (4.14) we also see that

$$a = 3^{\frac{1}{2}}(2/\pi)^{\frac{1}{3}} = 1{\cdot}4900. \tag{4·21}$$

At this point an arbitrary expression for ζ needs to be introduced, which will fix the complete figure in the ζ-plane. Our choice is

$$\left.\begin{aligned} \zeta &= \frac{aZ + 2bZ^2}{1 + cZ + bZ^2}, \\ \text{with} \quad c &= a + b - 1, \end{aligned}\right\} \tag{4.22}$$

which clearly complies with the four exact specifications listed above. The constant b is disposable, but only within certain limits recognized as follows. First, b must be real since the positive real axis of Z (i.e. the bottom in the physical plane) is mapped on the real axis of ζ between 0 and 2. Secondly, there obviously must be no pole of the expression (4.22) in the segment of the Z-plane mapping

the flow, nor should there be any zero (i.e. stagnation point) other than $Z = 0$. Thus b is required to be positive.

The third condition, which turns out to include the last, expresses the property proved in § 4.1: the free surface must fall steadily to its asymptotic level and not feature a trough. The slope $\tan\theta$ of the free surface is the same as $v/u = -\arg\zeta$ with $\arg Z = \frac{1}{3}\pi$, and accordingly we find from (4.22) that

$$\tan\theta = \frac{v}{u} = -\frac{\sqrt{3}\{a+2bR+b(2c-a)R^2\}}{a+2(ac-b)R+b(a+2c)R^2+4b^2R^3}, \tag{4.23}$$

where $R = |Z|$. This function has the required property (i.e. has no zero for $R < \infty$) only if

$$2c-a = a+2b-2 \geqslant 0.$$

Moreover, the equality must be excluded since the final convergence of the flow (for $R \to \infty$) would be too rapid in this special case (see below). Thus we must take

$$b > \tfrac{1}{2}(2-a) = 0{\cdot}2550. \tag{4.24}$$

When b is less than this value, the curved boundary in the ζ-plane makes a loop beyond the point $\zeta = 2$ and finally approaches it at an angle $-\frac{1}{3}\pi$ (i.e. $\arg(\zeta-2) \to -\frac{1}{3}\pi$ for $R \to \infty$). The corresponding angle is $\frac{2}{3}\pi$ when (4.24) is satisfied.

It appears reasonable to impose the further condition that $d(\tan\theta)/dR$, and hence the curvature of the free surface, should be of the same sign everywhere. The previous condition is obviously necessary to this property, but is insufficient. We see from (4.23) that the curvature would be negative just below the stagnation point, reversing sign farther down the surface, unless

$$ac-2b \geqslant 0,$$

that is, unless

$$b \leqslant a(a-1)/(2-a) = 1{\cdot}4316. \tag{4.25}$$

Now, a more detailed study of the flow in the vicinity of the stagnation point, when expressions like (4.19) are obtained to the next stage of approximation, shows that the dynamical boundary condition (4.14) requires $d(\tan\theta)/dR$ actually to vanish at $R = 0$. Thus the value $b = 1{\cdot}4316$ might seem to be the best choice. It is found, however, that this particular choice refines the description of the flow only very near to the stagnation point, and at undue expense of accuracy elsewhere. The criterion that finally decided the results to be presented below was the closeness of the approximation to (4.14) over the whole free surface, and the preceding discussion of conditions on b simply serves to rationalize the range of values $0{\cdot}2550 < b \leqslant 1{\cdot}4316$ that was tried.

There is one other definite property of the flow that can be checked against the approximate solution. Considering the final approach of the free surface to its asymptotic level far downstream, we may suppose that

$$y+\tfrac{1}{2} \sim e^{-\beta x} \quad \text{as} \quad x \to \infty. \tag{4.26}$$

where β is a positive real constant. From the linearized equations of steady motion, Lamb (1932, p. 407) has shown that

$$\frac{\tan\beta h}{\beta h} = F^2 \tag{4.27}$$

for any such exponential perturbation from a uniform stream with depth h and Froude number F. Taking the relevant values $h = \frac{1}{2}$ and $F = \sqrt{2}$, we find the smallest root of (4.27) to be $\beta = 2{\cdot}331$. Now, (4.23) shows that along the free surface

$$\frac{dy}{dx} \sim -\frac{\sqrt{3}(2c-a)}{4b}\frac{1}{R} \quad \text{as} \quad R \to \infty, \tag{4.28}$$

provided $2c - a \neq 0$ (cf. the remark immediately above equation (4.24)); and (4.15) shows that correspondingly

$$R \sim e^{\frac{1}{3}\pi\phi}. \tag{4.29}$$

We also have $\phi \sim 2x$ since $u = 2 + O(1/R)$. Hence, when these results are combined, the property (4.26) is seen to be provided by the proposed solution, but with $\beta = \frac{2}{3}\pi = 2{\cdot}094$ which is 10 % smaller than the correct value. This discrepancy seems quite tolerable, particularly as it is in a comparatively unimportant detail of the complete flow pattern.

We proceed to find the explicit form of the free surface corresponding to (4.22). From the definition (4.16) of ζ and then from the definition (4.15) of Z, it follows that

$$z = \int_i^w \frac{dw}{\zeta} = \frac{3}{\pi}\int_0^Z \frac{Z^2\,dZ}{\zeta(Z^3-1)}. \tag{4.30}$$

Upon the substitution of (4.22), this leads to

$$\begin{aligned} z &= \frac{3}{\pi}\int_0^Z \frac{\{Z + (a+b-1)Z^2 + bZ^3\}}{(a+2bZ)(Z^3-1)}\,dZ \\ &= \frac{1}{2\pi(a^2-2ab+4b^2)}\left[3a(2-a)\ln\left(1+\frac{2bZ}{a}\right)\right. \\ &\quad + 3(2b^2-ab+a)\ln(1-Z) + (2a^2-ab+2b^2-3a)\ln(1-Z^3) \\ &\quad \left. + 2\sqrt{3}(2b^2+ab-4b+a)\left\{\tan^{-1}\left(\frac{2Z+1}{\sqrt{3}}\right) - \frac{\pi}{6}\right\}\right]. \end{aligned} \tag{4.31}$$

Supplemented by the definition (4.15) of Z as a function of w, this result constitutes a solution for the whole flow in the form $z = f(w)$, from which the pattern of streamlines ($\psi = \text{const.}$ in $0 \leqslant \psi \leqslant 1$) could be constructed directly. The correct branch of the logarithms is made clear by reference to figure 10(*c*): for instance, the bottom $y = -1$ is given by taking Z real and $\geqslant 1$, with

$$\arg(1-Z) = \arg(1-Z^3) = -\pi.$$

To obtain parametric equations for the free surface, we put $Z = R\exp(\frac{1}{3}\pi i)$ in (4.31) and separate real and imaginary parts. The result is

$$\begin{aligned} x &= \frac{1}{4\pi(a^2-2ab+4b^2)}\left[3a(2-a)\ln\left(\frac{a^2+2abR+4b^2R^2}{a^2}\right)\right. \\ &\quad + 3(2b^2-ab+a)\ln(1-R+R^2) + 2(2a^2-ab+2b^2-3a)\ln(1-R^3) \\ &\quad \left. + 2\sqrt{3}(2b^2+ab+a-4b)\left\{\sin^{-1}\left(\frac{\sqrt{3}}{2\sqrt{(1-R+R^2)}}\right) - \frac{\pi}{3}\right\}\right], \end{aligned} \tag{4.32}$$

$$y = \frac{1}{4\pi(a^2-2ab+4b^2)}\left[6a(2-a)\tan^{-1}\left(\frac{\sqrt{3}bR}{a+bR}\right)\right.$$
$$+ 6(2b^2-ab+a)\tan^{-1}\left(\frac{\sqrt{3}R}{R-2}\right)$$
$$\left.+ \sqrt{3}(2b^2+ab+a-4b)\ln\left\{\frac{(1+R)^2}{1-R+R^2}\right\}\right]. \tag{4.33}$$

As R ranges from 0 to ∞, the $\sin^{-1}$ in (4.32) ranges from $\frac{1}{3}\pi$ to π, the first $\tan^{-1}$ in (4.33) from 0 to $\frac{1}{3}\pi$, and the second $\tan^{-1}$ from 0 to $-\frac{2}{3}\pi$.

R	x	$-y$	q^2	$\iota = -(q^2+8y)$
0·2	0·0068	0·0110	0·0864	0·0012
0·4	0·0291	0·0419	0·3324	0·0026
0·6	0·0681	0·0868	0·6928	0·0015
0·8	0·1214	0·1371	1·0971	−0·0005
1·0	0·1831	0·1852	1·4849	−0·0031
1·2	0·2474	0·2273	1·8244	−0·0063
1·4	0·3101	0·2623	2·1076	−0·0092
1·6	0·3693	0·2909	2·3387	−0·0111
1·8	0·4244	0·3143	2·5264	−0·0117
2·0	0·4752	0·3335	2·6794	−0·0111
2·4	0·5655	0·3628	2·9099	−0·0076
3·0	0·6781	0·3921	3·1366	−0·0001
4·0	0·8240	0·4208	3·3560	0·0107
5·0	0·9366	0·4376	3·4839	0·0173
10·0	1·2816	0·4699	3·7360	0·0232
50·0	2·0627	0·4942	3·9448	0·0085
100·0	2·3953	0·4971	3·9722	0·0045

TABLE 1

To check this result in the dynamical boundary condition (4.14), we also need to obtain from (4.22)

$$q^2 = |\zeta|^2 = \frac{R^2(a^2+2abR+4b^2R^2)}{1+cR+(c^2-b)R^2+cbR^3+b^2R^4}. \tag{4.34}$$

Values of q^2 given by (4.34) are to be compared with the corresponding values of $-8y$ given by (4.33). A helpful way to interpret the discrepancy is to suppose that a variable pressure $p = -\rho(\frac{1}{2}q^2+4y)$ is applied to the free surface. In this regard the solution as obtained is exact, and we gain an intuitive assurance that it is reliable if the modified physical system is made very close to the original one. It is meaningful, moreover, to express this pressure as a fraction of the pressure p_c in the cavity when the pressure at the upper boundary far upstream is zero; and, referring back to (2.2), we note that $p_c = \frac{1}{2}\rho c_1^2 = \frac{1}{2}$ in the present units. Thus we define

$$\iota = p/p_c = -(q^2+8y). \tag{4.35}$$

As explained earlier, these expressions have been computed with $a = 1{\cdot}4900$ and with various values of b in the range $0{\cdot}2500 < b \leqslant 1{\cdot}4316$. Over most of this range the graph of y *vs.* x suffers surprisingly little change and ι remains grati-

fyingly small. The best result appears to be obtained with $b = 0{\cdot}85$, and a selection of the numbers in this case is presented in table 1 to show the size of the error ι. Even when expressed as a fraction of q^2, which makes a more severe test, the difference between q^2 and $-8y$ nowhere rises above about 1 %. This result is plotted in figure 11, which is therefore presumably a very accurate picture of the free boundary of the energy-conserving flow.

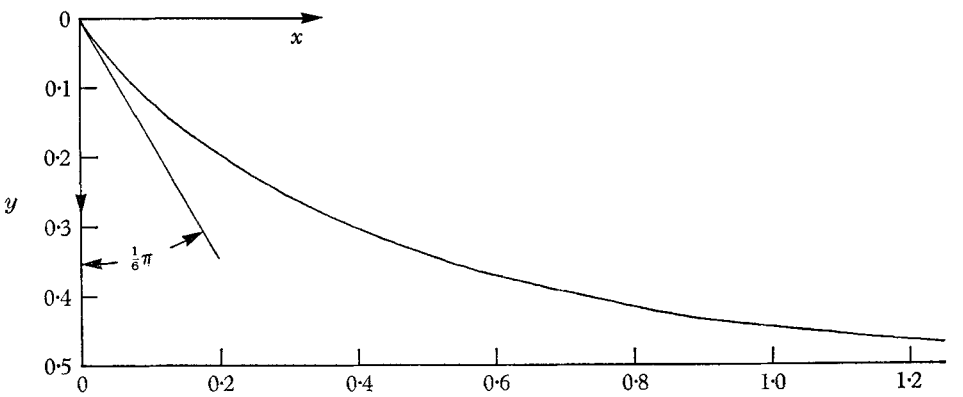

FIGURE 11. Calculated form of the free boundary.

5. Non-uniform asymptotic flows

Until now the investigation has been based on the assumption that the flow becomes uniform far downstream, and it remains to settle whether other asymptotic states might be possible. This question was raised by von Kármán (1940) in his discussion of gravity currents. He wrote, 'It is not known whether a mathematical analysis would lead to a surface approaching the horizontal level asymptotically or to waves with decreasing or constant amplitudes'.

The complete gamut of possible flows may be reviewed conveniently in a representation originally used by Benjamin & Lighthill (1954). Referring to steady, two-dimensional, perfect-fluid flow over a horizontal bottom and beneath a free surface, they based the representation on the following ideas: (1) For any *uniform* stream having velocity u, depth η and unit breadth, the discharge is $u\eta$, the total head measured above the bottom is $\eta + \frac{1}{2}u^2/g$, and the flow force is $\rho(\frac{1}{2}g\eta^2 + u^2\eta)$. (2) For the *critical* flow having the same discharge, the values of total head flow and force would be $\frac{3}{2}\eta_c$ and $\frac{3}{2}\rho g\eta_c^2$, where $\eta_c = \eta(u^2/g\eta)^{\frac{1}{3}} = \eta F^{\frac{2}{3}}$. (3) Dimensionless expressions for total head and flow force may be defined as the ratios of the actual to the latter values, thus

$$\left.\begin{aligned} r &= \frac{\eta(1+\frac{1}{2}F^2)}{\frac{3}{2}\eta_c} = \tfrac{2}{3}F^{-\frac{2}{3}} + \tfrac{1}{3}F^{\frac{4}{3}}, \\ s &= \frac{\eta^2(\frac{1}{2}+F^2)}{\frac{3}{2}\eta_c^2} = \tfrac{1}{3}F^{-\frac{4}{3}} + \tfrac{2}{3}F^{\frac{2}{3}}. \end{aligned}\right\} \tag{5.1}$$

(4) A plot of s against r according to (5.1) gives the cusped curve shown in figure 12: subcritical uniform flows ($F < 1$) are represented by points along the

upper branch, and supercritical ones ($F > 1$) along the lower. (5) Since total head and flow force are invariants of *any* steady flow in the absence of dissipation and of external horizontal forces, and since, moreover, their values determine the flow uniquely, therefore all possible flows of the type in question are represented separately by points in this diagram.

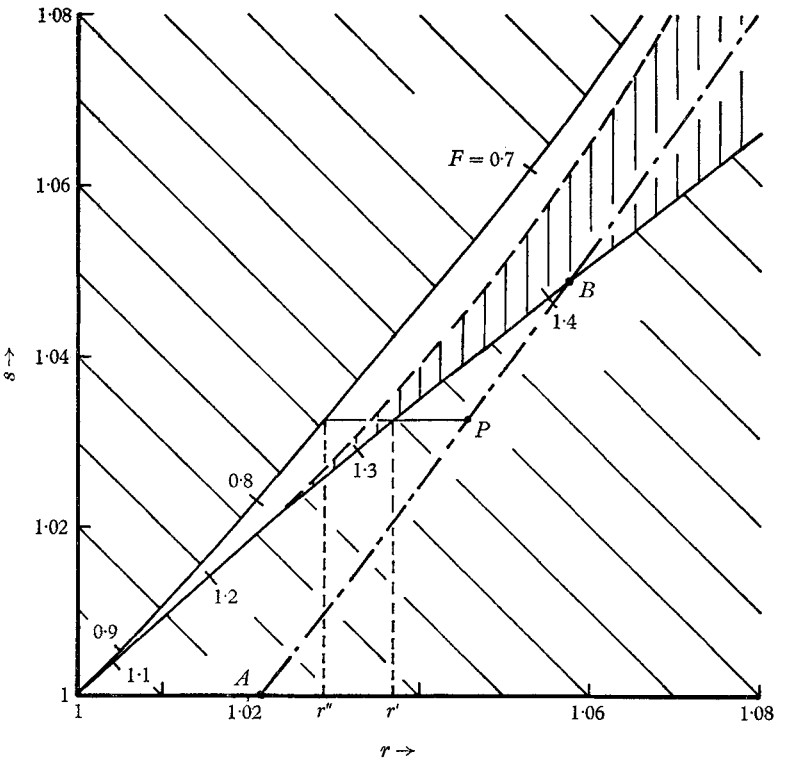

FIGURE 12. Energy-momentum diagram, after Benjamin & Lighthill (1954)

Benjamin & Lighthill showed that only points in the region enclosed by the cusped curve correspond to realizable wavetrains: the region outside (shaded by diagonal lines in figure 12) has no physical significance. Furthermore, a large part of the former region must be excepted since realization of the respective total-head and flow-force values is prevented by the breaking of waves. This part of figure 12 is shaded by vertical lines; and its upper boundary, drawn as a dashed curve, may be interpreted as the locus of 'waves of maximum height'—which have sharp crests at the stagnation level for the respective steady flow. The dashed curve starts on the lower branch of the cusped curve, at a point given by $F = 1{\cdot}25$ approximately, and approaches the upper branch asymptotically (for a complete discussion see De (1955), from which paper the present estimate of the dashed curve was obtained). Attempts to realize values of r and s in this excepted part of the diagram could only result as follows: either energy would be lost by breaking at the front of a wavetrain so that, as the flow became steady downstream, its state point (r, s) would be taken by the reduction of r up to or

beyond the locus of sharp-crested waves; or the wavetrain would be swept away downstream, leaving a uniform supercritical flow with (r, s) on the lower boundary of the excepted region.

The final point of interpretation needed is that points lying in the unshaded part of figure 12 represent only wavetrains with constant amplitudes. Under the required conditions of constant total head and flow force, there is no steady perfect-fluid flow in the form of an attenuating wavetrain. Thus one facet of the question posed by von Kármán is answered immediately: a solution featuring waves with decreasing amplitudes is impossible, and such a feature in practice could only be explained as an effect of friction.

To use the diagram for the present purpose, we recognize that values of r and s determining the receding flow must be matched upstream. There is, of course, no free surface upstream, but an equivalent open-channel flow must be evoked as the basis of the required definitions matching (5.1). The total head is simply the depth d (since O as indicated in figure 3 is a stagnation point); and for the critical flow having the prescribed discharge $c_1 d$, the total head would be $\frac{3}{2}df^{\frac{2}{3}}$, with $f = c_1/(gd)^{\frac{1}{2}}$. Hence we obtain

$$r = \tfrac{2}{3}f^{-\frac{2}{3}}. \tag{5.2}$$

Similarly, recalling the expression (2.4) for the flow force, we deduce that

$$s = \tfrac{1}{3}(f^{-\frac{4}{3}} + f^{\frac{2}{3}}), \tag{5.3}$$

and so

$$s = \frac{3r^2}{4} + \frac{2}{9r}. \tag{5.4}$$

This relationship between r and s is plotted as the chain-dotted curve in figure 12. (Let us call this the f-curve.)

Now, s has to be the same in all parts of the flow, since there is no external horizontal force to balance a change in flow force. But, to allow for the possibility of energy being dissipated at some stage before the flow reaches its final state downstream, we may, as in § 2.2, suppose a uniform loss of total head and so let the downstream value of r be smaller than the upstream value. Thus, respective to each upstream state represented by a point U on the f-curve, the possible states of flow downstream correspond to points to the left of P at the same distance from the r-axis.

On the f-curve the point A, at which $s = 1$, is given by $f = f_m = 0{\cdot}5273$, which is the maximum value of f found in § 2.2 (see (2.18) and its context). The only possibility downstream is then the critical flow represented by the cusp point, $r = s = 1$. Since $F = 1$ we have $h/d = f_m^{\frac{2}{3}}$, which reproduces the value $h/d = 0{\cdot}6527$ noted in § 2.2. And from (5.2) we find that $r = 1{\cdot}0214$ at A; hence the total-head loss represented by the jump from A is given by

$$\Delta = 0{\cdot}0214 \times 1{\cdot}5h = 0{\cdot}0209d,$$

which reproduces the maximum value noted above (2.21). For $f > f_m$, the f-curve lies wholly outside the quadrant $r \geqslant 1$, $s \geqslant 1$ shown in figure 12. The condition $f > f_m$ is physically impossible, therefore, since there is no realizable free-surface flow with $r < 1$ or $s < 1$.

Corresponding to every point P on the f-curve between A and B, there are two uniform flows possible downstream, which are represented by the two points on the cusped F-curve with the same s as P. A supercritical uniform flow is realized by a reduction in r to the value r' indicated in the figure, and a further reduction to the value r'' realizes a subcritical one. This situation has already been examined in § 2.2, where it was pointed out that the difference $r'-r''$ corresponds to the head loss in a hydraulic jump. It is possible that r could be reduced to an intermediate value within the width of the unshaded region of figure 12. A periodic wavetrain would then be produced, in just the way that Benjamin & Lighthill (1954) have explained in accounting for the undular form of weak hydraulic jumps and bores. However, smooth wavetrains are observed to be formed by hydraulic jumps only when F is less than about 1·25 and when the flow ahead is fairly even, whereas in the present situation a considerable amount of dissipation must first take place—presumably by breaking of the free surface—to realize a supercritical flow in this range of Froude number. It seems likely that the dissipative mechanism would proceed to consume all the available energy, not stopping at the stages where a uniform supercritical flow or a neighbouring state of wavy flow would evolve. Thus, as was argued from a complementary viewpoint in § 2, the uniform subcritical flows represented along the upper branch of the F-curve may in practice be the only steady flows obtainable for f-values (i.e. for particular propagation speeds) represented between the ends of the arc AB.

At the point B, and only at this point, the f-curve intersects the F-curve. This point represents the energy-conserving flow discussed in § 2.1, and it is given by the values $f = \frac{1}{2}$ and $F = \sqrt{2}$ that were presented as (2.9) and (2.10). We recall from § 2.1 that $h/d = \frac{1}{2}$ in this case. Also, the point to the left of B on the upper branch of the F-curve represents a subcritical flow with $h/d = 0{\cdot}7808$ (see (2.20)).

For $f < \frac{1}{2}$, the f-curve lies between the two branches of the F-curve. Then the uniform subcritical flows with particular s-values are still realizable by reductions in r, but the supercritical ones are impossible since in every case an increase in r (i.e. a supply of energy) would be needed to put the state point (r, s) for the receding stream on the lower branch. Referring back to figure 5 in § 2, we recognize that the possible flows are represented in the range $0{\cdot}7808 < h/d < 1$ of the figure, and the impossible ones would be represented in the range $0 < h/d < 0{\cdot}5$ given by a continuation of the figure to the left.

As regards the general question motivating this section of the paper, undoubtedly the most significant feature of figure 12 is that beyond B the f-curve passes into the region shaded by vertical lines, wherein the values (r, s) are excluded from realization by wave breaking. This shows that, at least in the range of the figure, no wavy flow is possible downstream without a considerable loss of energy occurring first. Thus the waveless flow studied in §§ 2.1 and 3 appears to be a unique solution to the present problem, under the specification that the motion is irrotational everywhere.

It remains to be confirmed, however, that the f-curve stays inside the region of breaking waves when extended far beyond the range of figure 12. As noted

previously, the upper boundary of this region (i.e. the locus of waves of maximum height) is asymptotic to the upper branch of the F-curve. But from (5.1) and (5.4) we find that the f-curve also approaches the upper branch asymptotically as $f \to 0$ and $F \to 0$, so that from the present viewpoint it cannot be settled whether or not the f-curve might finally cross into the unshaded region of the diagram. The extreme case in question is that where the downstream depth h greatly exceeds the depth $H = d - h$ of the cavity, and perforce the amplitude and wavelength of any waves that might be possible. These are 'surface waves', therefore, rather than the 'shallow-water waves' that are represented by discrete points in the Benjamin–Lighthill diagram. Taking the different approach that is needed for this case, we shall resolve the present issue in § 6.1 below.

6. The case of great depth

This case was touched upon at the end of § 2, where its importance with regard to gravity currents was emphasized. The depth d of the liquid upstream is considered to be very much greater than the mean depth $H = d - h$ of the cavity, so that it is H rather than d that must be taken as the basic length scale upon which the flow properties depend. As was pointed out in § 1, the outstanding fact in this case is that a net hydrostatic force acting horizontally has somehow to be balanced by a deficiency of momentum in the receding flow; and this requirement evidently cannot be met in the absence of dissipation if the free surface becomes flat asymptotically, since the hydrodynamic drag on a smooth 'half-body' is always zero (Prandtl & Tietjens 1934, § 78). The question raised just above, in the final paragraph of § 5, asks in effect whether a loss of momentum sufficient for the balance might occur as 'wave resistance', that is, by the formation of a *non-breaking* wavetrain.

The definite, negative answer to this question is deduced in the first of the following subsections. Then, by an argument recognizing the essentially dissipative character of the flow, an estimate of the velocity c_1 is obtained which confirms the tentative result noted at the end of § 2. This is compared in § 6.3 with various experimental results for gravity currents. Finally, in § 6.4, some observations are made concerning the form of the wake that must be left behind a breaking head wave.

6.1. *Is wave-breaking inevitable?*

The object is to test whether an irrotational flow is realizable having the characteristics illustrated in figure 13. The stagnation point O is taken as the origin of co-ordinates (x, y), with y drawn upwards. The total depth d is allowed to be finite for the purpose of the argument, but the limit $d \to \infty$ is to be taken finally.

Now consider the expression

$$S/\rho = -g \int y \, dy + \mathrm{Im} \int \tfrac{1}{2}\zeta^2 \, dz, \tag{6.1}$$

whose last part recalls the familiar theorem of Blasius in aerofoil theory (Lamb 1932, § 72*b*). Here $\zeta = u - iv$ is the function of the complex variable $z = x + iy$ that was defined generally by (4.16); and so, since there can be no pole of ζ^2 in the

flow domain, this expression evidently represents zero when the path of integration is any complete reducible circuit in this domain. Thus, writing the second integral in detail, we have that

$$S/\rho = \int \{-gy + \tfrac{1}{2}(u^2 - v^2)\}\, dy - \int uv\, dx \tag{6.2}$$

is zero when the integrals are taken around a closed path (i.e. a 'control surface' of unit span). We next note that $dx = (u/v)\, dy$ along any streamline; therefore, along the free surface in particular,

$$dS/dy = -\rho\{gy + \tfrac{1}{2}(u^2 + v^2)\} = 0 \tag{6.3}$$

in consequence of Bernoulli's theorem. It also appears from (6.2) that $dS = 0$ along a horizontal boundary. By an obvious application of these three facts, we conclude that S has the same value for *any* vertical section ($dx = 0$) extending

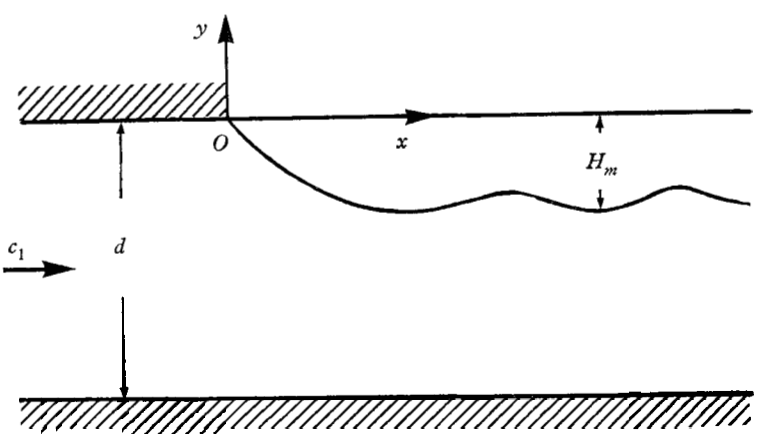

FIGURE 13. Illustration of contemplated wavy flow.

from the bottom $y = -d$ to the upper bounding streamline. Evaluated thus, (6.2) is an expression for flow force equivalent to the one used in §§ 2 and 5. But the concept of flow force may now be generalized to apply also to vertical sections terminated below by a horizontal plane inside the fluid: the last term in (6.2) is then needed to express the flux of horizontal momentum across this plane.

Equating the values of S for two complete sections, the first far upstream and the second a section where the depth of the free surface below O is H_m (see figure 13), we obtain directly

$$\tfrac{1}{2}c_1^2 H_m = -\tfrac{1}{2}gH_m^2 + \frac{1}{2}\int_{-d}^{-H_m} (2c_1 u' + u'^2 - v^2)\, dy, \tag{6.4}$$

where $u' = u - c_1$. But the condition of continuity gives

$$\int_{-d}^{-H_m} u'\, dy = c_1 H_m. \tag{6.5}$$

Hence there follows

$$H_m(gH_m - c_1^2) = \int_{-d}^{-H_m} (u'^2 - v^2)\, dy, \tag{6.6}$$

and the case $d = \infty$ is evidently covered by this result. [To remove possible doubt about the application when the depth is infinite, this case may be assumed from the start and the 'control surface' over which (6.2) is evaluated may be closed by a horizontal plane at some finite but large depth d'. Then a term $-\int uv\,dx$ is added to the right-hand side of (6.4), and a term $-\int v\,dx$ to the left-hand side of (6.5). But this first integral tends rapidly to equal c_1 times the second integral when d' is made large. Hence the result (6.6) is given as a limit when the range of integration is extended down to infinite depth. Essentially the same argument as this is used in the derivation of the familiar formula expressing aerodynamic drag in terms of wake velocity—see § 6.4 below.]

We now specify H_m to be a maximum, that is, the depth of a wave trough. Then $v = 0$ at the upper limit of the integral (6.6); and clearly v^2 can be made arbitrarily small over the whole vertical section by choosing a wave trough sufficiently far downstream, where the wavetrain must tend to a regular form. (Note that $v = 0$ everywhere under a trough in a strictly periodic wavetrain.) Thus we conclude that

$$gH_m > c_1^2 \tag{6.7}$$

if a steady wavetrain is to be possible.

In the limit of small wave amplitude, the velocity along the free surface must tend to equal c_1 far downstream when $d = \infty$; hence Bernoulli's theorem indicates the value $gH_m = \frac{1}{2}c_1^2$ which is less than half what is required by (6.7). The possibility of satisfying (6.7) appears, therefore, to depend only on waves of very large amplitude, for which the maximum depth H_m is considerably greater than the mean depth of the free surface. But the possible amplitude has the upper limit reached by waves of extreme form, whose crests rise to stagnation level and have sharp angles of 120° (Lamb 1932, p. 418). In the present system the stagnation level is the level of the upper horizontal boundary, so that for these waves H_m must be the same as the height between crests and troughs. Hence we can use directly the famous results calculated by Michell (1893) for these waves on deep water, their accuracy certainly being adequate for the present test.

Michell's estimate of the extreme height is

$$H_m = 0{\cdot}142\lambda, \tag{6.8}$$

where λ is wavelength; and the corresponding wave velocity is given by†

$$c_1^2 = 1{\cdot}20(g\lambda/2\pi). \tag{6.9}$$

Trying these values in (6·7) we find that the left-hand side is less than the right-hand side in the ratio $2\pi \times 0{\cdot}142/1{\cdot}20 = 0{\cdot}744$ to 1. Thus they fail to satisfy the inequality by a considerable margin.

The conclusion is that a smooth wavetrain is impossible and vigorous breaking is bound to occur around the first wave crest at the front of the cavity: that is, the breaking will occur on the rearward side of the head wave as we have previously defined it. By analogy, there must inevitably be breaking at the front of a

† In commenting upon this result Michell wrote inadvertently that the wave-velocity, rather than its square, is 1·20 times greater than in the case of infinitesimal amplitude, and this mis-statement was repeated by Lamb (1932, p. 418).

deeply submerged gravity current. The present inference as to the position of the breaking zone is indeed borne out by experimental observations on gravity currents (e.g. see Keulegan 1958, figure 28).

6.2. *The propagation velocity*

Following the indication of most observations on gravity currents, we may assume that behind the breaking zone in the present analogous system the free surface becomes more or less flat, so that the underlying mean flow is approximately parallel. The flow velocity cannot, however, have a uniform distribution with depth: instead, since liquid in the upper layers has suffered a considerable loss of total head in passing through the breaking zone, the velocity distribution will have the form of a wake, probably with its greatest 'defect' at the surface. It is a familiar and well-established fact that the piezometric pressure in a wake tends rapidly to become constant with increasing distance downstream, and this fact implies here that the level of the free surface will remain the same after a short distance from the region of establishment of the wake. These features are illustrated in figure 14.

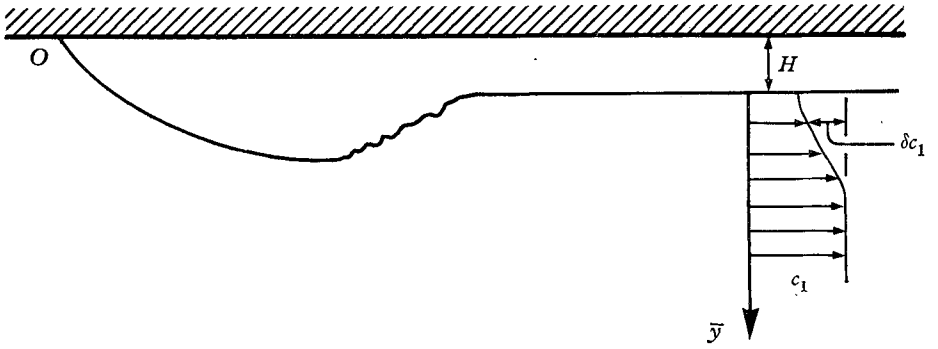

FIGURE 14. Illustration of real flow, showing breaking head wave and velocity profile of ensuing wake.

To find the velocity c_1 in terms of the mean depth H of the cavity, it is clearly inadequate to apply Bernoulli's theorem along the free surface, because the total-head loss cannot be specified. But the following argument leads to an estimate of c_1 that is independent of this unknown factor, and which therefore can be accepted with a fair measure of confidence. First, we consider that the flow up to the forward stagnation point is scarcely disturbed by the breaking process which, as experimental observation shows, generates intensive turbulence only on the rearward side of the head wave. Hence the pressure in the cavity, relative to the pressure on the horizontal boundary far upstream, is still given by $p_c = \frac{1}{2}\rho c_1^2$ as predicted hitherto. We next consider a path that is started at the boundary far upstream, is taken down to great depths, and finally is brought up to the free surface through the wake region where the flow is nearly parallel. In view of the property of constant piezometric pressure mentioned earlier regarding the wake, it is seen that everywhere along this path the pressure variation is simply hydrostatic; hence the pressure in the cavity is ρgH, corresponding to the net fall H

between the starting and end points. Thus, equating the two expressions for p_c, we have

$$c_1 = \sqrt{(2gH)}. \tag{6.10}$$

This result confirms the prediction made in the final paragraph of § 2. It is also equivalent to the result that von Kármán (1940) obtained by applying Bernoulli's theorem along the interface of a gravity current, overlooking the energy losses shown here to be essential. Stress must be laid on the fact that the agreement with his result is no more than a coincidence, since his reasoning was definitely wrong.

A few points of interpretation regarding the result (6.10) deserve to be noted, adding to the discussion in § 2. The simplest way to realize the envisaged flow would be to pump air into a cavity advancing along the upper, horizontal boundary of a deep expanse of liquid initially at rest. Then, as we have considered several times previously, this flow would be observed in a frame of reference moving steadily with the front of the cavity. If the air pressure p_c were fixed but its rate of supply unrestricted (e.g. by connecting the cavity to a large reservoir through a wide duct which offered little resistance to the air flow), then the velocity of the cavity is determined by $\frac{1}{2}\rho c_1^2 = p_c$ and (6.10) serves to predict its mean depth H. Alternatively, the supply rate $Q = c_1 H$ might be fixed (e.g. by throttling the air flow from a high-pressure reservoir), in which case (6.10) predicts $c_1 = (2gQ)^{\frac{1}{3}}$ and $H = (Q^2/2g)^{\frac{1}{3}}$. Also, the back-pressure exerted against the air supply would be $p_c = \rho(\frac{1}{2}g^2Q^2)^{\frac{1}{3}}$. Corresponding conditions can be envisaged for experiments on gravity currents. In several of the most informative series of experiments reported, however, precisely steady conditions were not achieved. In those of Keulegan (1958), for example, the rate of supply of salt water apparently diminished as the current progressed, so that the velocity and depth at the front gradually decreased. Nevertheless, on the supposition that the motion at the front was quasi-steady, a reasonable comparison can be made with the present theory (see below).

6.3. *Comparison with experiments on gravity currents*

The development of the theory in respect of the cavity flow is free from several obscurities that attend the application to gravity currents. In the former case the assumption of constant pressure over the free surface obviously gives an excellent approximation, and it is equally obvious that the free surface will emerge intact sufficiently far downstream: most of the air that may be entrained in the breaking zone will presumably be expelled within a short distance, just as in a hydraulic jump. But in a gravity current of, say, brine intruding into fresh water, the breaking process entails significant mixing of the two fluids and a consequent loss of definition of the interface downstream. Also, the heavier fluid in the head of the current is stirred vigorously, and so the assumption of constant piezometric pressure everywhere inside the current is not obviously well justified. Nevertheless, it seems fairly reasonable to suppose that any horizontal pressure gradient developed in the heavier fluid will be considerably smaller than the steep gradient of velocity head that the lighter fluid suffers in the breaking zone. On

this supposition, and on the understanding that H is to be measured to the densimetric mean level of the disturbed interface, the present estimate of the propagation velocity c_1 has an *a priori* foundation as before.

For application to gravity currents, the scaled form of (6.10) gives $\sqrt{2}$ as the value of the dimensionless coefficient

$$C_1 = \frac{c_1}{\sqrt{(\hat{g}H)}} \equiv \frac{c_1}{\sqrt{(gH\Delta\rho/\rho_2)}}. \tag{6.11}$$

In presenting his extensive series of experimental measurements on gravity currents, Keulegan (1958) listed values of such a coefficient, though with ρ_2 replaced by $\rho_m = \frac{1}{2}(\rho_1+\rho_2)$ in the definition. He also gave average values of this and other properties over two sets of data; but these values are not the most suitable for comparison with the theory, since the results averaged included many that evidently depended on the direct effect of viscosity, and also on the effect of the upper boundary. A fairer comparison is given by measurements listed in the last three rows of Keulegan's table 1, which relate to the largest density difference ($\Delta\rho/\rho_m = 0{\cdot}1168$) when the largest total depth of water was used ($d = 45{\cdot}5$ cm). Another listed measurement taken earlier in the same experiment is excluded because of its evidently greater dependence on the influence of the upper boundary and on transient effects (see the remark made two paragraphs above, following the first reference to Keulegan (1958)). From these results, when the small correction for the difference in definition is made, the average value $C_1 = 1{\cdot}20$ is obtained.

The discrepancy between this and the theoretical estimate $C_1 = 1{\cdot}414$ may be partly accountable to the effects of the upper boundary. From the experimental values of H, the average $H/d = 0{\cdot}111$ is found; and hence figure 7 in § 2 indicates that the propagation velocity is still significantly dependent on the presence of the upper boundary. With $H/d = 0{\cdot}111$, the formula (2.20) gives $C_1 = 1{\cdot}23$ which is encouragingly close to the experimental value. This estimate needs to be regarded with caution, however, because of the highly simplified physical basis of the analysis leading to (2.20).

While the grounds for selecting these particular experimental data appear quite reasonable, it must be acknowledged that the value of C_1 thus provided is distinctly larger than the estimates from most other available measurements on the speeds of gravity currents. Keulegan himself, considering the aggregate of all his many results, proposed $C_1 = 1{\cdot}07$ as a universal approximation applicable for Reynolds numbers ($R = c_1H/\nu$) greater than about 500, although he did note a slight tendency for C_1 to increase with Reynolds number. Again, Wood (1966) has reported numerous measurements of $c_1/(\hat{g}Q)^{\frac{1}{3}}$ giving a mean value of 1·06; and since this coefficient is equivalent to $C_1^{\frac{2}{3}}$, for present comparison his result amounts to $C_1 = 1{\cdot}09$. Middleton (1966) has also presented an extensive series of measurements, but, unfortunately for the purpose of comparison, he only recorded values of a dimensionless velocity coefficient based on the height of the head wave, say H_m, not on $H = Q/c_1$. His results give an average $c_1/(\hat{g}H_m)^{\frac{1}{2}} = 0{\cdot}75$, which agrees with Keulegan's 'universal' estimate of C_1 if, as Keulegan has suggested, H_m is taken generally to be about twice H (see below). In earlier measure-

ments by Braucher (1950), considerably smaller values of C_1 were observed, typically in the range 0·8–0·9. It appears, however, that the Reynolds numbers in these experiments were rather low, typically about 300, and evidently the effect of viscosity was dominant in determining the velocity of the front. In most of Keulegan's and Middleton's experiments the Reynolds numbers were at least one order of magnitude higher.

In view of the complex nature of the actual motion inside the front of a gravity current, the lack of a better general agreement with the predictions of the perfect-fluid theory seems hardly surprising, and from the present standpoint it would be profitless to pursue a more precise rationale for the available measurements of the propagation velocity. As a tentative suggestion in this direction, however, the following modification of the argument leading to (6.10) is perhaps worth mention. This recognizes that in practice the foremost point of a gravity current is not a stagnation point on the bottom as the theory predicts, but instead it lies at an appreciable height above the bottom and below it the interface folds backwards. This feature is shown in figure 1 and is common to all the observations cited in the first footnote to § 1. Let us suppose, accordingly, that a forward stagnation point exists at a height κH above the bottom, let us ignore the real-fluid effects that must inevitably bear on the interface below this level, and let us assume as before that a negligible change in piezometric pressure occurs inside the current at the stagnation level. Then the argument used previously leads to

$$C_1 = c_1/\sqrt{(\hat{g}H)} = \sqrt{\{2(1-\kappa)\}} \tag{6.12}$$

in place of (6.10). Considering, for example, certain of Middleton's results (1966, figure 3), one might take $\kappa = 0{\cdot}35$ as a reasonable estimate, whereupon (6.11) gives $C_1 = 1{\cdot}14$.

The set of experiments by Middleton (1966) is particularly informative as support for the applicability of present ideas to gravity currents moving down gradually sloping planes. First, the results presented in figure 3 of his paper show that the shape of the front remains practically the same over a range of slopes up to 0·06 (i.e. 3·4°). Secondly, it is demonstrated that the dimensionless velocity coefficient is also virtually independent of the slope, at least up to about 0·04 (see his table II and the relating discussion). A slight dependence was detected in some of the experiments, but in all cases the variation with slope was very much less than if the motion of the front were determined by a friction law of the Chézy type, such as might be supposed to apply at Reynolds numbers typical of the experiments. Lastly, and perhaps most tellingly, Middleton's paper presents a set of comparisons between the observed propagation velocity and the observed mean velocity of the uniform steady flow established eventually on the same slope by supplying the heavier fluid for long enough at the original rate. It is shown that, for the larger slopes considered, the former velocity was substantially less than the latter, in a ratio as small as 0·7 : 1, thus proving that the processes determining the progress of the front of a gravity current can be quite distinct from the balance of frictional forces that determines the ensuing uniform flow. That is, as was briefly explained in § 1, the front appears still to be driven primarily by excess hydrostatic pressure if the slope is small, and the

component of weight acting downhill is significant only in determining the steady flow that ensues if the original supply is maintained.

Another check on the theory is provided by Keulegan's measurements of the height of the head wave. Since it may be assumed that the flow is approximately irrotational as far as the crest of the wave (i.e. the trough in the cavity model), and since v is very unlikely to exceed the horizontal velocity perturbation u' anywhere in a vertical section passing through the crest, therefore the inequality (6.7) should apply to the wave. Thus we have

$$\left.\begin{aligned} H_m/H &> C_1^2 \quad \text{for all} \quad H/d, \\ &> 2 \quad \text{for} \quad H/d \to 0. \end{aligned}\right\} \tag{6.13}$$

All the results recorded by Keulegan (1958) comply with this theoretical condition, and the particular set of measurements considered above give the average $H_m/H = 2{\cdot}36$.

6.4. *Properties of the wake*

While the intensely turbulent motion in the zone of wave breaking is inaccessible to theoretical treatment, a few simple deductions regarding the ensuing wake can be made as follows. Referring to figure 14, we note that over two cross-sections respectively far upstream and downstream in the wake region, the pressure is everywhere hydrostatic except in the cavity where it has the constant value $p_c = \rho g H$. Hence a net horizontal force

$$P = \tfrac{1}{2}\rho g H^2 \tag{6.14}$$

acts in the direction from right to left in the figure. This force must be balanced by the hydrodynamic drag manifested in the momentum deficiency of the wake; and so, introducing a well-known formula for the drag (e.g. see Prandtl & Tietjens 1934, p. 125), we may write

$$P = \rho \int_0^\infty (c_1 - u)\, u\, d\bar{y} = \rho c_1^2 \int_0^\infty \delta(1-\delta)\, d\bar{y}, \tag{6.15}$$

where $\bar{y}$ denotes depth below the free surface in the wake region and where the horizontal mean velocity is expressed in the form $u = (1-\delta)c_1$. (The usual assumption is made here that, at the section where the integral is evaluated, the intensity of turbulence has diminished enough for the mean square of the velocity fluctuations to make no significant contribution to the total momentum flux.) When use is made of the result (6.10) for c_1, the combination of (6.14) and (6.15) gives

$$\int_0^\infty \delta(1-\delta)\, d\bar{y} = \tfrac{1}{4}H, \tag{6.16}$$

which implicitly relates the depth scale of the wake, expressed as a multiple of H, to the magnitude of the fractional velocity defect δ. It may be supposed that $\delta(\bar{y})$ is largest at the free surface $\bar{y} = 0$, and decreases steadily with increasing $\bar{y}$.

We now express the rate D at which energy is dissipated upstream from a particular section through the wake. The loss of energy per unit mass (i.e. of

total head times g) is $\frac{1}{2}(c_1^2-u^2)$; hence, in practical units, the dissipation rate is given by

$$D = \tfrac{1}{2}\rho\int_0^\infty (c_1^2-u^2)u\,d\bar{y} = \tfrac{1}{2}\rho c_1^3\int_0^\infty (2\delta-\delta^2)(1-\delta)\,d\bar{y}. \tag{6.17}$$

In view of (6.14), this expression can be arranged in the form

$$D = Pc_1 - \tfrac{1}{2}\rho c_1^3\int_0^\infty \delta^2(1-\delta)\,d\bar{y}, \tag{6.18}$$

whereupon (6.10) and (6.14) show that

$$D = \rho(\tfrac{1}{2}gH^5)^{\frac{1}{2}}\left\{1-\frac{2}{H}\int_0^\infty \delta^2(1-\delta)\,d\bar{y}\right\}. \tag{6.19}$$

At this point it must be recognized that the wake will gradually spread with increasing distance downstream, probably according to the same simple law that applies to two-dimensional wakes at large distances behind cylinders (cf. Prandtl 1952, p. 186; Goldstein 1938, § 252). Thus the depth scale, say L, ultimately increases in proportion to $x^{\frac{1}{2}}$; and correspondingly, as is indicated by (6.16), the maximum velocity defect $\delta(0)$ decreases in proportion to $x^{-\frac{1}{2}}$. However, the main interest of the preceding formulae lies in applying them fairly close to the head wave, say at distances $O(10H)$, where L is still comparable with the vertical scale of the wave-breaking zone. It seems reasonable to suppose that there is a considerable length over which the wake remains more or less in an 'original' form determined directly by the wave-breaking process, and that the eventual large-scale spreading occurs distinctly further downstream.

At sufficiently great distances the last term in (6.18) or (6.19) becomes insignificant, being proportional to $x^{-\frac{1}{2}}$, and thus $Pc_1 = \rho(\frac{1}{2}gH^5)^{\frac{1}{2}}$ is given as the total dissipation in the system. This confirms the result noted in the final paragraph of § 2, and it is obviously to be expected since Pc_1 is the energy input needed to drive the cavity into an expanse of stationary liquid. The last term in (6.18) or (6.19) must therefore represent the dissipation occurring downstream of the section at which the integral is evaluated. In particular, the second term within the braces on the right-hand side of (6.19) conveniently expresses this residual dissipation as a fraction of the total. Thus we are in a position to estimate an answer to the interesting question, what fraction of the total energy input is dissipated in the breaking zone?

To proceed, however, some arbitrary assumption must be made about the 'original' form of the function δ and, more crucially, the value of L/H must be guessed. For instance, let us take

$$\delta = \delta(0)\,e^{-\bar{y}/L}. \tag{6.20}$$

Then (6.16) gives $\quad \delta^2(0) - 2\delta(0) + \frac{1}{2}(H/L) = 0,$

and hence $\quad \delta(0) = 1-\{1-\frac{1}{2}(H/L)\}^{\frac{1}{2}}. \tag{6.21}$

Now, it has been shown that the depth of the head wave is somewhat greater than $2H$, and the breaking zone may be expected to cover most of its rearward side. At near distances downstream, therefore, the main part of the wake is likely to penetrate below the free surface to a depth roughly equal to H, and so $L/H = 1$

seems a reasonable guess. Accordingly, (6.21) indicates that $\delta(0) = 0{\cdot}3$ is perhaps a fair estimate of the velocity defect at the free surface a little way downstream. This figure implies that along the surface about half the original total head is lost in the breaking zone. Finally, putting (6.20) in (6.19) and then substituting the estimates of L/H and $\delta(0)$, we deduce that the dissipation occurring in the breaking zone is a fraction

$$1-(L/H)\{\delta^2(0)-\tfrac{2}{3}\delta^3(0)\} = 0{\cdot}93 \tag{6.22}$$

of the total.

[A possibly more attractive alternative would be to use the theoretical result

$$\left.\begin{aligned} \delta &= \delta(0)\{1-(\bar{y}/2L)^{\frac{3}{2}}\}^2 \quad \text{for} \quad 0 \leqslant \bar{y} \leqslant 2L, \\ &= 0 \qquad\qquad\qquad\quad \text{for} \quad \bar{y} \geqslant 2L, \end{aligned}\right\}$$

which satisfactorily approximates to the observed structure of the turbulent wake at large distances behind a symmetrical cylinder (Goldstein 1938, p. 584). This result is strictly justified only for fairly small values of $\delta(0)$, being derived on the assumption that the second term in the integral (6.15) is negligible; and so it would be consistent to simplify (6.16) in the same way, which leads to $\delta(0) = 0{\cdot}28(H/L)$. However, further discussion is unwarranted: the estimates depend very much less on the choice of form for δ than on the choice of L/H, the uncertainty of which precludes any improvement in precision.]

While the crudity of these numerical estimates must be recognized, there remains the advantage of the formulae (6.16) and (6.19) that they relate several properties to a single datum. If, for instance, the velocity of the free surface were measured experimentally so that the value of $\delta(0)$ were known, then one could make confident estimates of L and the proportions of the dissipation. As far as the writer is aware, no experimental study of this kind of cavity flow has yet been made; and unfortunately the available observations on gravity currents are of little avail as a test of the deductions in this subsection of the paper, which must be regarded as special to the cavity flow. In a gravity current, Reynolds stresses generated by the wave-breaking process are communicated across the interface to the heavier fluid, driving its upper layers into a rearward motion relative to the advancing front, and the turbulent boundary layer on the bottom is obviously similar in effect (cf. Bata & Bogich 1953). Thus the heavier fluid probably contributes significantly to the relative momentum of the wake, and probably also manifests a large part of the total dissipation.

7. Conclusion

This paper has, it is believed, more or less exhausted the useful applications of inviscid-fluid theory to steady gravity currents and to the related phenomena that have been pointed out. This aim focuses only, of course, on one narrow aspect of the general subject; for it must be acknowledged that gravity currents in practice are highly complex phenomena, generally featuring a great deal of turbulence and significant mixing of the two fluids, so that the interpretation of them depends vitally on semi-empirical analyses in the province to which Keulegan has been the outstanding contributor. But the present work serves at

least to explain some broad principles underlying what is observed, in particular showing the essential role of wave-breaking and the energy losses thereby enforced.

A number of attractive experiments are suggested by this theoretical discussion, some of them being of such simplicity that the writer must apologize for not trying them himself and reporting the outcome here. For instance, the energy-conserving flow discussed in §§ 2.1 and 4 could be modelled by allowing liquid to run out freely from a long horizontal box of rectangular cross-section, and a photograph of the free surface in profile could be compared with the theoretical curve in figure 11. Also, the interesting effects predicted in § 2.2 to be the result of throttling the air flow into the cavity could be checked, probably quite easily. It would be of particular interest to see whether, as the theory indicates, the speed of advance of the cavity can be increased by this means.

I am grateful to Dr J. F. Davidson for drawing my attention to the neat hydrodynamical problem treated in §§ 2.1 and 3 of the paper: the entire investigation owes to the original stimulus of discussing this problem with him. This work was done in the Institute of Geophysics and Planetary Physics during a visit supported by the U.S. Office of Naval Research under Contract Nonr-2261(29) and by the U.S. National Science Foundation under Contract GP-2414

REFERENCES

BATA, G. & BOGICH, K. 1953 Some observations on density currents in the laboratory and in the field. *Proc. Minn. Internat. Hydraulics Conv., Univ. of Minnesota*, p. 387.

BENJAMIN, T. B. & LIGHTHILL, M. J. 1954 On cnoidal waves and bores. *Proc. Roy. Soc.* A **224**, 448.

BERSON, F. A. 1958 Some measurements on undercutting cold air. *Quart. J. Roy. Meteorol. Soc.* **84**, 1.

BINNIE, A. M. 1952 The flow of water under a sluice-gate. *Quart. J. Mech. appl. Math.* **5**, 395.

BRAUCHER, E. P. 1950 Initial characteristics of density current flow. S.M. Thesis, Massachusetts Inst. of Technology.

CLARKE, R. H. 1961 Mesostructure of dry cold fronts over featureless terrain. *J. Meteorology*, **18**, 715.

DE, S. C. 1955 Contributions to the theory of Stokes waves. *Proc. Camb. Phil. Soc.* **51**, 713.

GOLDSTEIN, S. (Ed.) 1938 *Modern Developments in Fluid Dynamics.* Oxford University Press. (Dover edition, 1965.)

IPPEN, A. T. & HARLEMAN, D. R. F. 1952 Steady-state characteristics of subsurface flow. *Proc. NBS Symp. on Gravity Waves, Nat. Bur. Stand. Circ.* **521**, 79.

KÁRMÁN, T. VON 1940 The engineer grapples with nonlinear problems. *Bull. Am. Math. Soc.* **46**, 615.

KEULEGAN, G. H. 1949 Interfacial instability and mixing in stratified flows. *J. Res. Nat. Bur. Stand.* **43**, 487.

KEULEGAN, G. H. 1957 An experimental study of the motion of saline water from locks into fresh water channels. *Nat. Bur. Stand. Rept.* 5168.

KEULEGAN, G. H. 1958 The motion of saline fronts in still water. *Nat. Bur. Stand. Rept.* 5831.

KEUNEN, P. H. 1950 Turbidity currents of high density. 18*th Internat. Geol. Congr., London, Repts.* Pt. 8, p. 44.

LAMB, H. 1932 *Hydrodynamics*, 6th ed. Cambridge University Press. (Dover edition, 1945.)

MICHELL, A. G. M. 1893 The highest waves in water. *Phil. Mag.* (v), **36**, 430.

MIDDLETON, G. V. 1966 Experiments on density and turbidity currents. 1. Motion of the head. *Canad. J. Earth Sci.* **3**, 523.

PRANDTL, L. 1952 *Essentials of Fluid Dynamics*. New York: Hafner.

PRANDTL, L. & TIETJENS, O. G. 1934 *Applied Hydro- and Aerodynamics*. New York: McGraw-Hill. (Dover edition, 1957.)

SCHIJF, J. B. & SCHÖNFELD, J. C. 1953 Theoretical considerations on the motion of salt and fresh water. *Proc. Minn. Internat. Hydraulics Conv., Univ. of Minnesota*, p. 321.

SOUTHWELL, R. V. & VAISEY, G. 1946 Relaxation methods applied to engineering problems. XII: Fluid motions characterized by 'free' streamlines. *Phil. Trans. Roy. Soc.* A **240**, 117.

WOOD, I. R. 1966 Studies in unsteady self preserving turbulent flows. *Univ. of New South Wales, Water Research Lab., Rept.* no. 81.

YIH, C.-S. 1947 A study of the characteristics of gravity waves at a liquid interface. M.S. Thesis, State Univ. of Iowa.

YIH, C.-S. 1965 *Dynamics of Nonhomogeneous Fluids*. New York: Macmillan.

ZUKOSKI, E. E. 1966 Influence of viscosity, surface tension, and inclination angle on motion of long bubbles in closed tubes. *J. Fluid Mech.* **25**, 821.